Immunobiology 224 (2019) 270–284

Contents lists available at ScienceDirect

Immunobiology

journal homepage: www.elsevier.com/locate/imbio

Enhancing the pro-inflammatory anti-cancer T cell response *via* biomanufactured, secretome-based, immunotherapeutics

Xining Yang[a,b], Ning Kang[b,c], Wendy M. Toyofuku[b,c], Mark D. Scott[a,b,c,*]

[a] Department of Pathology and Laboratory Medicine, University of British Columbia, Vancouver, BC, V6T 1Z3, Canada
[b] University of British Columbia Centre for Blood Research, Canada
[c] Canadian Blood Services, Canada

ARTICLE INFO

Keywords:
T lymphocyte
Secretome
Pro-inflammatory
Cancer
miRNA

ABSTRACT

T lymphocytes play a critical role in the pro-inflammatory anti-cancer response; hence, significant pharmacologic efforts have been made to enhance the endogenous T cell response. Unfortunately, significant toxicity arises consequent to pan T cell activation. In contrast, the less robust T cell alloresponse has also demonstrated an anti-cancer effect, but poses an inherent risk of GvHD. To overcome the GvHD risk, an acellular pro-inflammatory agent (IA1) has been biomanufactured from the secretome of the allorecognition response. To assess IA1's immunomodulatory activity, T cell proliferation and differentiation were determined *in vitro*. The pro-inflammatory properties of the IA1 therapeutic were mediated by the miRNA-enriched fractions. Moreover, cross-species efficacy was observed consequent to the evolutionary conservation of miRNA. IA1 exerted no toxicity to resting PBMC but induced significant proliferation of resting $CD3^+$ ($CD4^+$ and $CD8^+$) T cells and skewed the response towards a pro-inflammatory state (*i.e.*, increased Teff:Treg ratio). Crucially, IA1-activated PBMC demonstrated a potent inhibition of cancer cell (HeLa and SH-4 melanoma) proliferation relative to the resting PBMC. The anti-proliferation effect of IA1-activated PBMC was noted within ~12 h *versus* 4–5 days for resting cells. A second biomanufactured therapeutic (IA2; produced using HeLa cells) surprisingly demonstrated direct toxicity to cancer cells but was less effective than IA1 in inducing a cell-mediated response. This study demonstrates that miRNA-enriched therapeutics can be biomanufactured from the secretome and can induce a potent pro-inflammatory, anti-cancer, effect on resting lymphocytes.

1. Introduction

An individual's immune system is a continuous balancing act between tolerance and inflammation.(Rabinovich and Toscano, 2009) Cancers may occur when this balance is skewed towards a tolerogenic state consequent to the loss of the inflammatory response to abnormal cells.(Kasiske et al., 2004) This immunological tenet is clearly supported by the finding that immunocompromised individual (either inherent or drug induced) have a higher incidence of cancers.(Dunn et al., 2006; Le Mire et al., 2006) Despite the potential role of a nonresponsive immune environment, most anti-cancer therapeutics have historically been cytotoxic drugs.(Gascoigne and Taylor, 2009) These cytotoxic drugs typically targeted all proliferating cells; thus killing not only the cancer cell but also other proliferating cells (including immune cells further depressing the immune response) leading to significant toxicity to normal cells and tissues.(Lee and Margolin, 2011) Consequent to this problem, research and clinical efforts have more recently focused on enhancing the individuals own immune response to cancer cells.

The T lymphocyte (T cell) plays a critical role in the anti-cancer inflammatory responses. An effective anti-cancer pro-inflammatory T cell response is dependent upon the activation of effector T cells (Teff) which include: $CD8^+$ cytotoxic T lymphocytes (CTL) and $CD4^+$ T helper cells (Th) such as Th1 and Th17. Normally, lymphocytes are activated upon ligation of their antigen receptors with specific cognate antigens.(Cantrell, 2002) However, because of the low frequency of antigen-specific lymphocytes, as well as difficulty in identification and isolation, research initially focused on the use of agents that directly activated T cells in the absence of antigens. This approach is exemplified by the nonspecific activation of T cells *via* mitogens (*e.g.*, phytohemagglutinin; PHA), cytokines (*e.g.*, IL-2), or monoclonal

Abbreviations: SYN, Syngenic or autologous secretome derived therapeutic; IA1, Inflammatory Agent 1; IA2, Inflammatory Agent 2; TA1, Tolerogenic Agent 1

* Corresponding author at: Canadian Blood Services and the Centre for Blood Research, University of British Columbia, Life Sciences Centre, 2350 Health Sciences Mall, Vancouver, BC, V6T 1Z3, Canada.
E-mail address: mdscott@mail.ubc.ca (M.D. Scott).

https://doi.org/10.1016/j.imbio.2018.12.003
Received 14 September 2018; Received in revised form 17 December 2018; Accepted 18 December 2018
Available online 28 December 2018

antibodies (*e.g.*, anti-CD3 and anti-CD28). However, consequent to the overly robust T cell response arising from these pan-T cell agents, a cytokine release syndrome was often induced leading to multi-organ failures, severe morbidity and increased mortality leading to the suspension or abrogation of multiple clinical trials.(Larsson and Coutinho, 1979; Liao et al., 2011; Trickett and Kwan, 2003; Suntharalingam et al., 2006; Han and Takita, 1972; Maciel et al., 1976) More recently, to improve antigen specificity, chimeric antigen receptor T cell (CAR-T) therapy has been developed and shown to be a highly promising approach to enhancing the endogenous immunological response to cancers. However, while highly effective, clinical studies have similarly shown significant adverse effects (*e.g.*, cytokine release syndrome) leading to enhanced morbidity and mortality.(Bonifant et al., 2016) Additionally, CAR-T therapy is expensive with costs approaching $500,000 (US) per patient.(Bach et al., 2017) Thus, alternative approaches to activate the endogenous T cell response in a controlled manner, with less toxicity, and improved affordability are needed.

Multiple studies suggest that a strong T cell-mediated ($CD4^+$ and $CD8^+$) alloresponse can promote an effective anticancer response. (Fabre, 2001; Barrett, 1997; Bian et al., 2013; Barrett and Childs, 2000; Renga et al., 2003; Eljaafari et al., 2006) In contrast to pan-T cell activators (*e.g.*, mitogens; anti-CD3/CD28), the allorecognition response is more limited as only 1–10% of T cells are alloresponsive.(Nisbet et al., 1969; Abul et al., 2015) However, despite the 'low' number of potentially reactive cells, the infusion of significant numbers of allogeneic donor cells is beset by a significant risk of morbidity and mortality due to Graft *versus* Host Disease (GvHD) thus limiting its practical applicability. However, by using a 'secretome approach', acellular conditioned media can be prepared that have tissue specific biologic activity.(Beer et al., 2016; Lichtenauer et al., 2011; Mildner et al., 2013; Di Santo et al., 2009; Lee et al., 2015) While the active components within the secretome were traditionally viewed as paracrine factors (*e.g.,* cytokines), the secretome contains a variety of biologically active components that include proteins, lipids, microRNA (miRNA) as well as extracellular vesicles (exosomes and microparticles).(Beer et al., 2016; Yao and Asayama, 2017; Beer et al., 2015; Haider et al., 2015; Simader et al., 2017) Not surprisingly, the secretome components released are defined by their cell/tissue origin as well as the physiologic activation state of the cells.(Di Santo et al., 2009; Lee et al., 2015; Dowling and Clynes, 2011; Sholl-Franco and Araujo, 1997) Consequently, secretome conditioned media can be designed to exert differential biologic responses.(Kang et al., 2017; Wang et al., 2011, 2015) Indeed, previous studies from our laboratory using human or murine mixed lymphocyte reaction (MLR) models demonstrated that we could generate either tolerogenic or pro-inflammatory secretomes (*i.e.*, conditioned media) by regulating the strength of the allorecognition response.(Kang et al., 2017; Wang et al., 2011, 2015; Kyluik-Price et al., 2014; Kyluik-Price and Scott, 2016; Le and Scott, 2010; Murad et al., 1999)

Using a pro-inflammatory, lymphocyte-allorecognition, secretome approach, we hypothesized that the anti-cancer efficacy of resting peripheral blood mononuclear cells (PBMC) could be significantly enhanced. As demonstrated in this study, secretome biotherapeutics can be reproducibly biomanufactured. The allorecognition-based Inflammatory Agent 1 (IA1) was found to be a potent activator of resting human PBMC promoting proliferation of both $CD8^+$ CTL and $CD4^+$ Teff cell proliferation. The essential acellular effectors of the secretome were soluble and exosome encapsulated miRNA and, due to the conserved nature of miRNA, demonstrated cross-species efficacy. Significantly, the proliferation induced by IA1 was approximately 50% that of the allogenic response and dramatically less than that induced by mitogens (PHA) or monoclonal antibodies (anti-CD3/anti-CD28) suggesting that systemic toxicity, relative to these agents, should be significantly reduced. Importantly, IA1 exerted no direct toxicity to PBMC. However, as will be demonstrated, IA1-treatment of resting PBMC resulted in a significantly enhanced anti-cancer effect relative to untreated or sham-miRNA treated donor matched PBMC. Concurrent studies were similarly done using a lymphocyte-cancer cell (HeLa) secretome biotherapeutic (IA2). As shown in this study, IA1 and IA2 demonstrated significant biologic and anti-cancer differences. Successful development of this novel secretome therapeutic approach may prove useful in enhancing the endogenous immune response to cancer and in reducing the metastatic potential of existing cancers consequent to enhanced immunosurveillance.

2. Methods and materials

2.1. General methods

2.1.1. Human PBMC

All human experiments were done in accordance with the University of British Columbia Clinical Research Ethics Board and the Code of Ethics of the World Medical Association (Declaration of Helsinki). Following informed written consent, donor whole blood was collected in heparinized Vacutainer® blood tubes (BD, Franklin Lakes, NJ). PBMC were prepared using Histopaque-1077 (Sigma-Aldrich, St. Louis, MO) as per the product instructions. The PBMC layer was washed twice with 25 mM HEPES/RPMI 1640 (with L-glutamine; Invitrogen by Life Technologies, Carlsbad, CA) containing 0.01% human albumin (Sigma-Aldrich, St. Louis, MO). Human PBMC were suspended in the appropriate media as needed for biomanufacturing of IA1, cell phenotyping and cell proliferation assays.

2.1.2. Statistical analysis

All data were expressed as mean ± standard error mean (SEM). A minimum of three independent experiments were performed in duplicates for all studies. Data analysis was conducted using GraphPad Prism 6.0 (GraphPad Software, Inc., San Diego, CA). For significance, a minimum p value of < 0.05 was used. For comparison of two means, an independent t-test was performed. For comparison of three or more means, a one-way analysis of variance (ANOVA) was performed. When significant differences were found, a post-hoc Tukey test was conducted for pair-wise comparison of means. For all studies significance was denoted as: * $p < 0.05$; ** $p < 0.01$; *** $p < 0.001$; and **** $p < 0.0001$.

2.2. Biomanufacturing of acellular biotherapeutics

Production of the alloresponse-based acellular Inflammatory Agent 1 (IA1; Fig. 1A) was done using the secretome obtained from *in vitro* human two-way MLR as previously described.(Kang et al., 2017; Wang et al., 2011, 2015) In brief, the allogenic preparation IA1-Allo (IA1) was manufactured using PBMC from two MHC-disparate human donors suspended in AIM V media (research grade; ThermoFisher Scientific, Grand Island, NY). A final of 1×10^6 total PBMC from each donor were plated in multiwell flat-bottom 24-well tissue culture plates (BD Biosciences, Discovery Labware, Bedford, MA). Production of the cancer cell-stimulated secretome biologic IA2 (IA2-HeLa) was done using a modified MLR in which one PBMC donor was replaced with cultured (allogenic) HeLa cells (PBMC:HeLa reaction; Fig. 1A). In brief, freshly isolated human PBMC were co-cultured with HeLa cells at a ratio of PBMC:HeLa = 50:1 in 24-well tissue culture plates. The final total PBMC number was 1×10^6. The negative control Syngenic (SYN) secretome was prepared from untreated single donor PBMC seeded at 2×10^6 cells per 24-well plate well. For some studies, the relative effects of the pro-inflammatory IA1 and IA2 were compared to our previous described Tolerogenic Agent 1 (TA1) preparation.(Wang et al., 2015) TA1 manufacturing was accomplished using an *in vitro* human mPEG-MLR as previously described.(Kang et al., 2017; Wang et al., 2011, 2015; Kyluik-Price et al., 2014; Kyluik-Price and Scott, 2016; Le and Scott, 2010; Murad et al., 1999; Wang et al., 2012) In brief, PBMC from one of the human donors were derivatized using 20 kDa succinimidyl valerate activated methoxypoly (ethylene glycol) (SVA-mPEG;

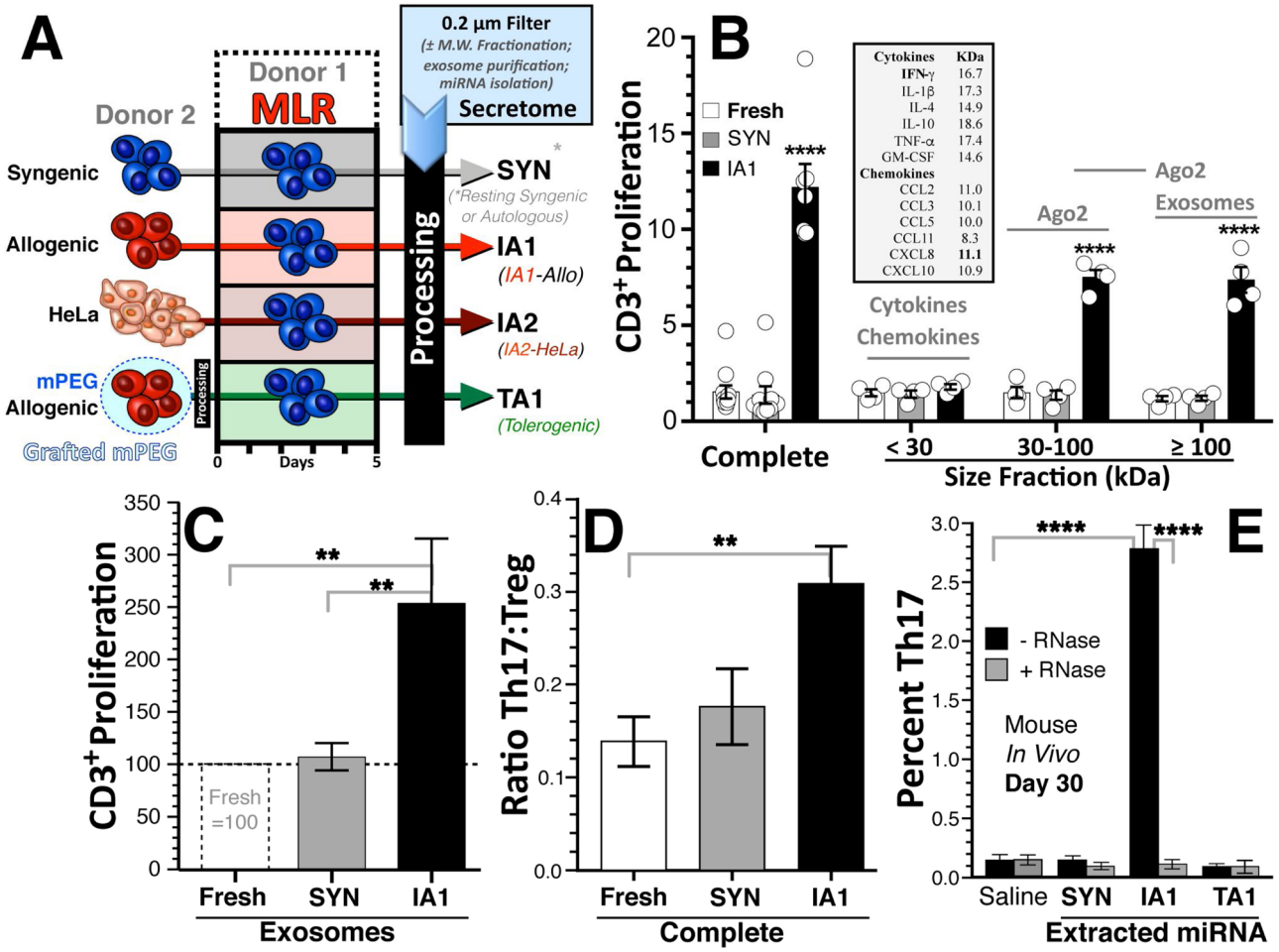

Fig. 1. Allogeneic MLR-based secretome biomanufacturing process and immunomodulatory effects. **Panel A:** Manufacturing scheme of secretome biotherapeutics. SYN was derived from resting PBMC while IA1 was produced using an allogenic MLR. IA2 was derived from a PBMC-HeLa cell coculture. TA1 was manufactured form a mPEG-MLR in which one donor population was modified with methoxy(polyethylene glycol). Secretomes were collected at day 5 and further processed *via* centrifugation and 0.2 µm ultrafiltration. For some experiments, additional processing steps included size fractionation, exosome purification and miRNA isolation. **Panel B:** The T lymphocyte ($CD3^+$) proliferative potential of IA1 was assessed for both complete IA1 and M.W. restricted subfractions (< 30, 30–100 and ≥100 kDa). Shown is the CFSE proliferation of $CD3^+$ T cells measured at day 10 *via* flow cytometry. The proliferative potential of IA1 was not associated with the cytokine-rich fraction, but was solely observed in the high molecular weight, miRNA-containing, fractions. The table insert indicates the M.W. of representative cytokines and chemokines. Results of independent experiments are shown using white circles. **Panel C:** Only IA1 exosomes induced $CD3^+$ T cell proliferation. Exosomes from fresh PBMC were normalized to 100%. **Panel D:** Analysis of subset differentiation of resting PBMC demonstrated that only IA1 induced a pro-inflammatory state as defined by the Th17:Treg ratio at 10 days post treatment. **Panel E:** Supporting the potential *in vivo* use of IA1, mice treated with miRNA prepared from IA1, but not SYN or TA1, had significantly elevated Th17 levels at 30 days post *i.v.* administration. However, RNase treatment of the IA1-miRNA abolished all immunomodulatory activity. **Panels B–E** show the mean ± SEM. Significance was calculated in comparison to fresh unless otherwise specified. For all studies significance was denoted as: * $p < 0.05$; ** $p < 0.01$; *** $p < 0.001$; and **** $p < 0.0001$. N ≥ 4 for all samples.

Laysan Bio Inc. Arab, AL) at a grafting concentration of 2.0 mM per 4×10^6 cells/ml. Post-production processing and utilization of TA1 was otherwise identical to that of IA1. In all experiments, the indicated secretome(s), or secretome derived products, were compared to control cells treated with fresh media (denoted as 'Fresh').

Following extensive optimization studies, all conditioned media were collected at 5 days post plating. Post collection, the media was processed *via* centrifugation (400 × *g*; 10 min) to remove cells and cellular debris followed by ultrafiltration using a 0.2 µm syringe filter (Pall Corporation, Port Washington, NY). In some studies, the media was further processed as described below. The processed media were aliquoted and stored in the -80 °C freezer. Studies (not shown) demonstrated that freezing and thawing had no significant impact on the immunomodulatory activity of the processed media. For tissue culture studies, the processed media were mixed 1:1 with fresh media and then seeded with the indicated cells.

2.2.1. Molecular weight fractionation

To characterize the active component(s) of the acellular media, size fractionation studies were done using the Amicon® Ultra-0.5 ml 30/100 kDa fractionation tubes (EMD Millipore, Billerica, MA). Previous studies have similarly used molecular weight fractionation to generate miRNA-enriched fractions (> 90 kDa; based on molecular weight of the miRNA containing Ago2 and exosomes). (Arroyo et al., 2011; Turchinovich and Burwinkel, 2012) In contrast, the majority of cytokines and chemokines resides in the < 30 kDa fraction (Fig. 1B) allowing for the delineation of their role in the IA1 secretome.(Stenken and Poschenrieder, 2015) Briefly, complete media was centrifuged at 14,000 × g for 15 min to collect the filtrate. Another 2 min of 1000 × g spin was conducted to recover the concentrated solute. The immunomodulatory activity of both the filtrate and the concentrate were assessed on resting human PBMC using a 1:1 dilution with fresh media as described above. To assess the role of cytokines and chemokines in the pro-inflammatory and anti-cancer effects of IA1, the proliferative

effects of the cytokine rich fraction (< 30 kDa) was compared to complete media and ≥30 kDa fractions.

2.2.2. Exosome preparation and analysis

While significant amounts of stable, non-complex/encapsulated miRNA are found within the media, additional miRNA are bound to higher molecular weight Ago2 (˜97 kDa) and in very large exosomes. To assess the role of exosome encapsulated miRNA, exosomes were purified from the processed media using the Total Exosome Isolation Kit (Cat. No. 4,478,359; Invitrogen by Life Technologies, Carlsbad, CA). Briefly, the indicated acellular preparations were mixed with the Total Exosome Isolation reagent and incubated at 4 °C overnight followed by centrifugation (10,000 × g; 1 h at 4 °C). The pelleted exosomes were resuspended in a sufficient volume of fresh, cell specific, tissue culture media to the volume of initial acellular product. To control for the potential xeno-stimulation of the IA1-human exosomes, exosomes from the human SYN secretome were used as controls in the cross-species stimulation studies as they expressed the same xenoantigen disparity as the IA1-derived exosomes.

2.2.3. Functionality of isolated secretome miRNA

To further assess the potential role of miRNA, miRNA from the SYN, IA1 and TA1 secretome media were isolated using the mirVana™ PARIS™ kit (Cat. No. AM1556, Ambion, Life Technologies; Grand Island, NY). Following processing, the highly enriched small RNA fraction containing miRNA was prepared.(Wang et al., 2015) To confirm that miRNA was the active component, RNase A was used to degrade the nucleic acid. To assess the immunomodulatory activity of the miRNA preparations (± RNase treatment), BALB/c mice were treated (*i.v.* 200 µl/mouse; N = 5/group) with either the control or RNase-treated (50 ng RNase A; 10 min at 37 °C; Life Technologies) miRNA and Th17 levels were assessed at Day 30 post treatment. All murine studies were performed following protocol approval by the University of British Columbia Animal Care Committee and were done in accordance with the Canadian Council of Animal Care guidelines.

2.2.4. Effect of IA1/IA2 activation on lymphocyte miRNA expression

Total RNA was extracted from resting PBMC ± treatment (SYN, IA1, IA2, TA1, anti-CD3/anti-CD28 and PHA) following 72 h incubation using the mirVana™ PARIS™ kit (Ambion, Life Technologies, Grand Island, NY). Following processing, the highly enriched small RNA fraction containing miRNA was prepared using RNase/DNase free water. Total cellular RNA of the samples was prepared using the Agilent RNA 6000 Nano Kit (Cat. No. 5067-1511;). Sample RNA concentration and quality (*e.g.*, integrity) was assessed using the Agilent 2100 Bioanalyzer System (Agilent Technologies, Santa Clara, CA). Samples were stored at -80 °C until further use. To partially characterize and quantify the relative abundance the miRNA species present in the resting and differentially activated PBMC, quantitative reverse transcription polymerase chain reaction (qRT-PCR) was done using the miScript miRNA PCR Array system (Qiagen, Frederick, MD) for the human immunopathology pathway. These miRNA microarrays plates were run using an Applied Biosystems StepOnePlus™ Real Time PCR System (ThermoFisher Scientific, Grand Island, NY). This human immunopathology array plate is pre-configured with the appropriate RNA and quality controls and has been validated by Qiagen. This array profiles the expression of 84 miRNA differentially expressed during normal and pathological immune responses. It is worth noting that the 84 miRNA examined are not all inclusive and that other miRNA are likely to be present and could be of immunoregulatory importance. Threshold and baseline were defined and the resultant C_t (threshold cycle) values were calculated using the StepOnePlus software (v.2.1). C_t values were exported and analyzed using the Qiagen GeneGlobe Online Analysis Center using the Relative Quantification qRT-PCR method for analysis ($\Delta\Delta C_t$). The data shown represent three biological replicates analyzed independently by qRT-PCR.

2.2.5. Cross-species efficacy

Because miRNA are evolutionarily conserved, the cross-species efficacy of human- and murine-sourced IA1 on murine splenocytes and human PBMC was examined. All murine studies were done in accordance with the Canadian Council of Animal Care and the University of British Columbia Animal Care Committee guidelines and were conducted within the Centre for Disease Modeling at the University of British Columbia. For production of murine IA1, two MHC (H-2) disparate allogenic strains of mice were used: BALB/c, H-2d; and C57BL/6, H-2b. Murine splenocytes were prepared from freshly harvested spleen *via* homogenization into a cell suspension in PBS with 0.2% bovine serum albumin (BSA; Sigma-Aldrich, St. Louis, MO) using the frosted end of two microscope slides. Red blood cells were removed by treating splenocytes using BD Pharm Lyse buffer (BD Pharmingen, San Diego, CA). *In vitro* production of murine IA1 was done as described above for the human IA1 except for resuspending cells in RPMI 1640 media supplemented with 10% heat-inactivated Fetal Bovine Serum (FBS; Gemini Bio-Products, West Sacramento, CA), 1% L-glutamine, 1% penicillin-streptomycin and ß-mercaptoethaniol (50 µM). Resting human PBMC and murine splenocytes were treated with human- and murine-sourced IA1 respectively. Cell proliferation and the Th17:Treg ratio were determined as described below. In addition, the effects of exosomes isolated from human IA1 on murine splenocytes were similarly examined.

2.3. Comparative effects of IA1 and IA2 to existing T cell activation approaches

2.3.1. Effect of IA1 on lymphocyte viability

To determine whether IA1 exerted direct toxicity to treated cells, 7-amino-actinomycin D (7 AAD; BD Biosciences, San Jose, CA) viability studies were done. 7 AAD is a fluorescent nucleic dye that is excluded from viable cells but can enter non-viable cells due to increased membrane permeability. Cells were stained with 7 AAD at a final concentration of 0.05 mg/ml and incubated at room temperature for 15 min prior to flow cytometric analysis as previously described.(Kang et al., 2017)

2.3.2. Effect of IA1 on T cell proliferation and phenotyping

In vitro cell proliferation was assessed *via* flow cytometry using the CellTrace CFSE (carboxyfluorescein diacetate succinimidyl ester) Cell Proliferation Kit (Cat. No. C34554i; CellTrace, Molecular probes, Invitrogen, Eugene, OR). Human PBMC labeling was done according to the product insert at a final concentration of 2.5 µM CFSE per 2×10^6 cells total. In some studies, the effects of IA1 induced proliferation relative to control MLR, mitogen stimulation, and anti-CD3/anti-CD28 induced proliferation were compared.

The T cell lymphocyte subpopulations ($CD3^+CD4^+$ and $CD3^+CD8^+$) were measured by flow cytometry using fluorescently labeled anti- CD3, CD4 and CD8 monoclonal antibodies (mAb; BD Pharmingen, San Jose, CA). Human Th17 and Treg subsets were measured using the BD Th17/Treg Phenotyping Kit (Cat. No. 560,762; BD Biosciences, San Jose, CA). The inflammatory Th17 lymphocytes were $CD3^+CD4^+IL\text{-}17^+$ while T regulatory lymphocytes (Treg) were $CD3^+CD4^+Foxp3^+$. After the staining, the cells (1×10^6 total) were washed and resuspended in phosphate buffered saline (PBS with 0.5% BSA) prior to flow acquisition. Unstained controls were used to determine background fluorescence. The role of Th17 cells in disease (both as causative Teff and in the anti-cancer response) has evolved significantly over the last several years and may be underestimated due to Treg-Th17 plasticity.(Wang et al., 2015; Punt et al., 2015a, b; Wilke et al., 2011; Ye et al., 2013) Because of interrelationship between Th17 and Treg cells, the ratio (Th17:Treg) of the two populations serves as an excellent surrogate for assessing the inflammatory state. Indeed, as demonstrated in the NOD mouse, Th17 cells were more closely aligned with both the onset and prevention of Type 1 diabetes.(Wang et al.,

2015) All samples were acquired using the FACSCalibur flow cytometer and CellQuest Pro software (BD Biosciences, San Jose, CA) for both acquisition and analysis.

2.3.3. Comparison of IA1 to Allorecognition and Pan T cell activation agents

As previously noted, past clinical studies have examined the anti-cancer utility of allo-based and direct T cell (anti-CD3/anti-CD28 and mitogen) activation therapies. Hence, the resting PBMC proliferation potential of IA1 was compared to MLR-based alloproliferation, anti-CD3/anti-CD28 and phytohemagglutinin (PHA; mitogen) stimulation. Allorecognition-based proliferation assays (MLR) were conducted as described above. For anti-CD3/anti-CD28 activation assays, freshly isolated human PBMC were stimulated with plate-bound anti-human CD3e (5 μg/ml; BD Pharmingen, San Diego, CA), in the presence of soluble anti-human CD28 (1 μg/ml; BD Pharmingen, San Jose, CA). After 3 days incubation, the T cell proliferation and differentiation were assessed *via* flow cytometry. For mitogen stimulation studies, PBMC were treated with phytohemagglutinin (PHA, Sigma-Aldrich, St. Louis, MO) at an amount of 2 μg per 1×10^6 total cells; following 4 days incubation, T cell proliferation and differentiation were measured by flow cytometry. Additionally, the effect of the tolerogenic miRNA–Based TA1 preparation was done for comparative purposes.

2.4. Anti-cancer efficacy of IA1- and IA2- activated PBMC on cancer cell proliferation

2.4.1. Cancer cell lines

To investigate the anti-cancer effects of IA1 and IA2, human cancer cell proliferation assays were conducted using HeLa and SH-4 melanoma cell lines. HeLa cell line (CCL-2) was purchased from ATCC and cultured under 5% CO_2 in Dulbecco's modified eagle's medium (DMEM; high-glucose contains 4.5 g/l D-glucose, without L-glutamine or sodium pyruvate; Invitrogen, Carlsbad, CA) supplemented with 10% heat-inactivated FBS, 10 mM HEPES, 100U penicillin and 100 μg streptomycin (Invitrogen, Carlsbad, CA). Human melanoma SH-4 cell line (CRL-7724) was purchased from ATCC and cultured under 5% CO_2 in DMEM supplemented with 10% heat-inactivated FBS, 4 mM L-glutamine, 1 mM Na pyruvate, 100U penicillin and 100 μg streptomycin (all from Invitrogen, Carlsbad, CA). Both cell lines were used at ~80% confluence.

2.4.2. Inhibition of cancer cell proliferation

The direct toxicity and anti-proliferative effects of control and secretome-treated (SYN, IA1, IA2 and TA1) PBMC against the HeLa (epithelial) and SH-4 (melanoma) human cancer cell lines were assessed using an ACEA iCELLigence instrument (ACEA Biosciences, Inc., San Diego, CA). The iCELLigence provides a continuous, real-time, measurement of cell proliferation using changes in the electrical impedance within tissue culture wells. The change in impedance is induced by the increase in adherent cells and is unaffected by cells (*e.g.,* PBMC) that remain non-adherent. All studies were done with an initial seeding density of 5000 HeLa, or 20,000 SH-4, cells per well of the ACEA E-8 electronic microtiter plate in DMEM medium with an acclimation time for initial adherence for 60 min. Cells were incubated in the iCELLigence instrument maintained at 37 °C in a humidified 5% CO_2 incubator for 7 days. Direct toxicity of the secretome products (added 1:1 into DMEM) was assessed by measuring HeLa/SH-4 cells proliferation in the absence of PBMC. The effect of resting and secretome-activated PBMC on cancer cell proliferation was assessed by overlaying the PBMC onto the seeded cancer cells at 60 min. Sufficient PBMC were added to the wells to achieve Effector:Target ratios of 0:1, 10:1, 25:1 and 50:1. The relatative efficacy of the SYN, IA1, IA2 and TA1 activated PBMC were then compared. In some HeLa cell experiments, the inhibition of cancer cell proliferation by purified (resting and activated) $CD4^+$ and $CD8^+$ T cells was assessed. Purified populations of $CD4^+$ and $CD8^+$ T cells were obtained from resting PBMC using a Dynabeads® Untouched™ Human CD4 or CD8 T Cell Isolation Kit (Cat. No. 11352D and 11348D, respectively; Invitrogen by Life Technologies, Carlsbad, CA) according to the manufacturers instructions. The purified (≥90%) T cells were pretreated with the acellular secretome products (SYN, IA1 and IA2) for 24 h and then overlaid on cancer cells with cell proliferation being measured continuously for 7 days (168 h).

2.4.3. Lymphocyte:Tumor conjugation

An important mechanism in the lymphocyte-mediated killing of cancer cells is direct cell:cell interaction. To quantitatively assess this interaction, flow cytometric cell conjugation assays were done. Briefly, PBMC or HeLa cells were stained with amine reactive fluorescent probes at a final concentration of 0.5 μM CFSE (PBMC) or 0.2 μM Far Red-DDAO (HeLa; CellTrace, Molecular Probes, Invitrogen, Eugene, OR) per 2×10^6 cells, respectively. Cells were washed 3 times in excess RPMI 1640 media to remove any unincorporated stain. Stained PBMC and HeLa cells were co-cultured in RPMI 1640 media at a ratio of PBMC:HeLa = 50:1 to a final concentration of 1×10^6 cells/ml. Co-cultures were centrifuged briefly at 100 × g, 4 °C for 1 min and incubated at 37 °C for 20 min to allow conjugation of cells. Cells were fixed by addition of 2% methanol-free formaldehyde. The double-stained cell population ($CFSE^+$Far Red-$DDAO^+$) was examined to determine the percentage of cell conjugation using flow cytometry as previously described.

In addition to the conjugation assay, time-lapse photographies of the PBMC:HeLa cell co-cultures were captured. PBMC and HeLa cells (seeded at 5000 total) were co-cultured in RPMI 1640 media supplemented with 25 mM HEPES and 0.01% human albumin, at a ratio of PBMC:HeLa = 50:1, in a heated (37 °C) humidity chamber (Becton Dickinson, Franklin Lakes, NJ). Photomicrographs were taken at 20X magnification every 10 s for 90 min using a Nikon Eclipse Ti microscope mounted with a camera (Digital sight DS-U3) and analyzed using NIS-elements software. Representative photos at specific time points were then extracted for presentation.

3. Results

3.1. Proliferation and differentiation effects of IA1 and IA2 on resting $CD3^+$ T cells

Previous studies have demonstrated that an allogenic cell-mediated immune response can exert a significant anti-cancer effect; albeit with a risk of GvHD to the recipient.(Fabre, 2001) To circumvent the GvHD risk, our laboratory has utilized an acellular cocktail derived from the secretome (*i.e.,* conditioned media) of an allogenic MLR. As diagrammatically shown in Fig. 1A, acellular cocktails were prepared from syngenic (*i.e.,* resting cells; SYN), allogenic (IA1), allogenic-HeLa (IA2) and tolerogenic (TA1) cell culture systems after a 5 days' reaction. The TA1 preparation, previously shown to inhibit alloproliferation and to increase Tregs and reduce Teffs, was derived from an allogenic MLR in which one MHC-disparate population was modified by grafting mPEG to the cells.(Wang et al., 2011, 2015) To determine if a pro-inflammatory response could be induced by these acellular cocktails, resting PBMC were treated with the various indicated preparations. As demonstrated in Fig. 1B, the IA1, but not SYN, induced a significant ($p < 0.0001$) increase in resting $CD3^+$ T cell proliferation at day 10 of treatment. Previously we hypothesized that soluble cytokines contained in the IA1 or TA1 conditioned media mediated their respective immunomodulatory effects.(Wang et al., 2011, 2015) However, size fractionation studies of the complete secretomes (Fig. 1B) found that the cytokine/chemokine rich fraction (< 30 kDa) exhibited no proliferative effect on $CD3^+$ T cells. In contrast, higher molecular weight fractions containing the Ago2/miRNA complex (~97 kDa) and miRNA-rich exosomes (≥100 kDa) retained significant proliferative activity relative to the complete IA1 supporting earlier findings of biologic activity for exosomes.(Arroyo et al., 2011; Valadi et al., 2007) Of note, if

miRNA are purified (using the mirVana™ PARIS™ kit) from the secretome, the immunomodulatory activity resides within the < 10 kDa fraction which contains the miRNA. (Wang et al., 2015) In contrast, the similarly sized fractions from the Fresh and SYN demonstrated no proliferative activity. Moreover, exosome isolation studies demonstrated that IA1, but not the SYN, exosomes induced resting PBMC proliferation (Fig. 1C). Importantly, IA1 not only increased $CD3^+$ T cell proliferation (Fig. 1B) but also increased the Teff:Treg ratio (Th17:Treg) resulting in a pro-inflammatory environment; crucial for cancer cell killing (Fig. 1D). Also of note, IA1 exerted an immunomodulatory effect *in vivo*. Mice treated with miRNA extracted from IA1 exhibited significantly elevated Th17 levels even 30 days post *i.v.* administration (Fig. 1E). Further suggesting a central role for secretome miRNA, RNase-treatment of the extracted IA1-miRNA prior to its administration obviated its *in vivo* immunomodulatory effect. In contrast, SYN had no effect on proliferation, Teff:Treg ratio, or *in vivo* murine Th17 cells levels relative to fresh media or saline treatment. The tolerogenic TA1 was characterized by decreased Teff and increased Treg cells (data not shown). (Wang et al., 2011, 2015)

In contrast to protein-based signals (*e.g.* cytokines and chemokines), miRNA are highly conserved evolutionarily with well-established cross-species, and even cross-kingdom, efficacy.(Liang et al., 2013) To further confirm the role of miRNA in the pro-inflammatory effects of IA1, cross-species (Human ↔ Mouse) studies were conducted using resting human PBMC and murine spleoncytes. As expected, human-sourced IA1 induced a significant proliferation of resting human $CD3^+$ T cells (Fig. 2A). Importantly, murine-sourced IA1 also induced proliferation ($p < 0.05$) of human $CD3^+$ T cells. More dramatically, human IA1 stimulated a significant proliferation ($p < 0.0001$) of murine splenocytes at a level comparable to murine-sourced IA1 (Fig. 2B). It must be noted that the murine fresh and SYN did somewhat elevate human and murine $CD3^+$ proliferation over the expected baseline levels; perhaps due to the ongoing immune events within the donor mice. Importantly, in the context of cancer cell killing, the proliferation induced by the IA1 preparations (human and murine) resulted in a pro-inflammatory shift in the Th17:Treg ratio both intra- and inter-species (Fig. 2**C-D**). Of interest, the murine IA1 induced a larger increase ($p < 0.05$) in the human Teff:Treg ratio than did the human IA1. In mouse splenocytes, both the murine and human IA1s were comparably effective at increasing the Teff:Treg ratio relative to the resting and SYN-treated samples. Moreover, human IA1-exosomes similarly showed cross-species efficacy on murine $CD3^+$ T cell proliferation. As shown in Fig. 2E, as expected, murine IA1-exosomes induced murine $CD3^+$ T cells proliferation and, in accordance to what was observed in Fig. 2B, human IA1-exosomes induced an even more potent increase in murine $CD3^+$ T cell proliferation than did the murine IA1-exosomes. Human SYN-exosomes exerted no proliferative effect while murine SYN-exosomes showed a modest increase in proliferation similar to that observed with murine SYN-media (Fig. 2B). Hence, acellular miRNA–Based preparations derived from an MLR can be used to induce a pro-inflammatory T cell response while obviating the risk of GvHD.

3.2. Comparative effects of IA1 and IA2 to existing T cell activation approaches

A previous problem with T cell activation (*e.g.*, mitogens and mAb) strategies has been an overly robust response. (Suntharalingam et al., 2006) Hence, we examined the comparative proliferative efficacy and differentiation profiles of IA1 relative to that of potent T cell activators such as anti-CD3/anti-CD28 and PHA. Moreover, we also tested a PBMC-cancer cell (HeLa; Fig. 1A) generated preparation denoted as IA2 to determine if a cancer cell specific agent would prove more efficacious than IA1. As shown in Fig. 3A, the differential effects of IA1 and IA2 on $CD3^+$, $CD4^+$ and $CD8^+$ T lymphocytes were compared to that observed in a control MLR as well as direct mAb (anti-CD3/anti-CD28) or mitogen (PHA) stimulation. Both IA1 and IA2 significantly increased the $CD3^+$ T cell proliferation in resting PBMC (12.2 ± 1.21% and 10.7 ± 0.47%, respectively), and this increase encompassed both $CD4^+$ and $CD8^+$ T cells. Interestingly, IA1 predominantly increased $CD4^+$ while IA2 predominantly increased $CD8^+$ T cell proliferation suggesting compositional and mechanistic differences between the two preparations. As anticipated, the acellular IA1 and IA2 induced proliferation of resting PBMC was slightly less than 50% of that observed in a control two-way MLR (30.9 ± 3.41%) where two MHC-disparate populations are both proliferating. In contrast, anti-CD3/anti-CD28 and PHA resulted in very high levels of $CD3^+$ proliferation (78.1 ± 1.78% and 94.4 ± 0.27%, respectively). Indeed, these overly robust responses are indicative of the adverse clinical events associated with mitogen/mitogen-like therapeutics.(Suntharalingam et al., 2006) Therefore, IA1 and IA2 increased resting $CD3^+$ T cell proliferation in a more restrained manner than allo- (*i.e.*, MLR), anti-CD3/anti-CD28, or PHA stimulation. In contrast to IA1, the TA1 treatment had no proliferative effects on $CD3^+$, $CD4^+$ and $CD8^+$ T cell proliferation relative to the resting and SYN-treated cells. Indeed as shown previously, TA1 shrank pro-inflammatory subsets and dramatically decreased the Th17:Treg ratio rescuing NOD mice from the development of Type 1 diabetes.(Wang et al., 2015) Not only did IA1 and IA2 induce differential proliferation of $CD4^+$ and $CD8^+$ T cells, they also altered the $CD4^+$ subset (Th17 and Treg) differentiation pattern (Fig. 3B). IA1 significantly increased both Th17 and Treg, but the increase in Th17 was predominant resulting in an increased Th17:Treg ratio (2.21-fold, $p < 0.05$). In contrast, IA2 expanded Th17 moderately but significantly shrank the Treg population; the loss of Tregs further elevated the Th17:Treg ratio (4.43-fold, $p < 0.0001$). Therefore, while IA1 exhibited a pro-inflammatory Teff:-Treg ratio similar to an MLR, IA2 demonstrated a more significant increase ($p < 0.01$) in the Th17:Treg ratio.

However, in cancers, the immune system is not in a “resting” state (*i.e.*, as modeled by resting PBMC used above) and, while ineffective at the gross level, will exhibit some degree of immune activation. To determine if IA1 could further enhance, or jumpstart, an existing immune response, MLR studies were conducted in the absence and presence of the SYN and IA1 preparations. As shown in Fig. 4**A–B**, IA1 greatly enhanced the alloresponse within an MLR as demonstrated by human $CD3^+$, (**Panels A–B**) $CD4^+$ and $CD8^+$ (**Panel B**) T cell proliferation. In contrast, SYN-treated MLR exhibited no significant changes in $CD3^+$ or $CD4^+$ T cell proliferation relative to the control MLR. However, a slight, but statistically ($p < 0.05$) significant, increase in $CD8^+$ T cell proliferation relative to the control MLR was observed. Interestingly, in contrast to a $CD4^+$-centric T cell proliferative response in resting PBMC, IA1 had a greater proliferative effect on $CD8^+$ T cells ($p < 0.0001$ relative to $CD4^+$ T cells) in the MLR allorecognition model. Within the $CD4^+$ T cells, IA1 significantly increased Th17 cells relative to the control MLR while Treg cells remained statistically unchanged (Fig. 4C). Interestingly, the SYN actually decreased Th17 cells ($p < 0.05$) but had no effect on Treg cells. Consequently, as shown in Fig. 4D, the Th17:Treg ratio of the control MLR was significantly increased (1.55-fold; $p < 0.01$) by IA1 further supporting its role as a potential pro-inflammatory agent. In contrast, the SYN preparation significantly decreased (0.59-fold; $p < 0.05$) the Teff:Treg ratio. Hence, these findings suggested that IA1 could enhance the anti-cancer T cell mediated immune response.

3.3. Anti-cancer efficacy of IA1- and IA2- activated PBMC on cancer cell proliferation

The anti-cancer efficacy of IA1 and IA2 activated T lymphocytes was assessed using two *in vitro* cancer models (HeLa and SH-4 cell lines). Of biologic significance, neither the IA1 or IA2 preparations exerted direct toxicity to resting PBMC following 24 h of exposure (Fig. 5A). Indeed, the viability of the resting PBMC was slightly, but statistically significantly ($p < 0.0001$) increased, with both therapeutics. Moreover, IA1 and IA1-activated lymphocytes demonstrated minimal bystander

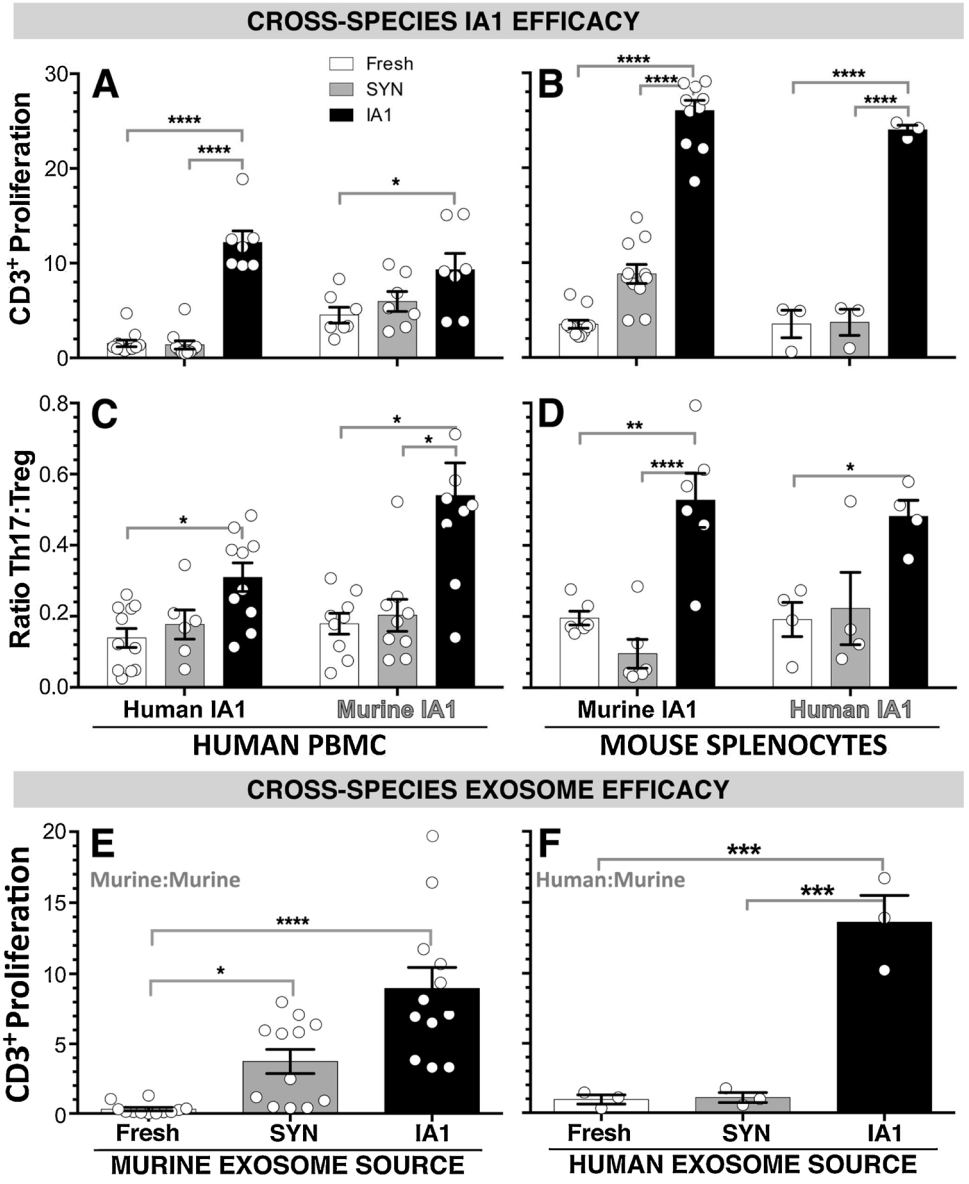

Fig. 2. IA1 and IA1-derived exosomes demonstrate cross-species efficacy on resting human and murine CD3$^+$ T lymphocyte proliferation and subset differentiation. **Panels A–B:** Proliferation (CFSE) of resting human and murine CD3$^+$ T lymphocytes (10 and 7 days, respectively) treated with human- or murine-sourced Fresh, SYN and IA1. **Panels C-D:** Effects of IA1 on the Th17:Treg ratio of human and murine CD4$^+$ T lymphocytes at day 10 or 7; respectively. **Panels E-F:** Murine resting splenocytes were treated with either murine- (E) and human-sourced (F) exosomes for 7 days. IA1, but not fresh or SYN, exosomes demonstrated significant proliferative effects and cross-species efficacy. Shown are the mean ± SEM. Significance was calculated in comparison to fresh unless otherwise specified and denoted as: * $p < 0.05$; ** $p < 0.01$; *** $p < 0.001$; and **** $p < 0.0001$. N ≥ 3 for all samples.

toxicity to primary, non-cancerous, cells *in vitro* (*e.g.,* murine myoblasts; data not shown). To assess the anti-cancer efficacy of IA1 and IA2, cancer cell growth over 7 days was followed using a real-time proliferation assay. Similar to its effect on PBMC, IA1 (as well as the SYN and TAI) had no direct toxicity to HeLa cells (Fig. 5B). Surprisingly however, direct treatment of HeLa cells with IA2 demonstrated an almost total inhibition of growth. Indeed, by approximately 30 h, no Hela cell proliferation was noted in HeLa cell cultures treated directly with IA2. The direct toxicity of IA2 to HeLa cells (Fig. 5B), but not PBMC, suggested a pro-apoptotic or necrotic effect on the HeLa cells that was not induced by IA1.

To examine the effect of IA1 and IA2 (as well as the SYN and TA1) on the ability of resting PBMC to recognize and attenuate cancer cell growth, resting human PBMC were treated with the therapeutic cocktails for 24 h, washed, and overlaid on the HeLa cells at ratios of 0:1, 25:1 and 50:1 (PBMC:HeLa; Figs. 5**C-D**). In the absence of PBMC, HeLa cells showed continuous growth over 5–6 days (Fig. 5**B–H**). Addition of untreated, but allogenic, resting PBMC resulted in some growth retardation by day 4 and the eventual killing of the HeLa cells beginning at approximately day 4 or 5 consequent to allorecognition and an anti-HeLa response. The SYN treated PBMC behaved similarly. In contrast, IA1 pretreated PBMC demonstrated a significantly enhanced anti-HeLa effect at both the 25:1 (**Panel C**) and, most significantly, 50:1 (**Panel D**) ratios. Moreover, as also shown in Fig. 5**C-D**, IA2 pretreated PBMC exerted an even more potent (relative to IA1) anti-HeLa effect at both ratios; though it was actually less than the direct toxicity (* dotted line) of IA2 to HeLa cells. Of interest, treatment of allogenic PBMC with the tolerogenic TA1 demonstrated no anti-HeLa effect; in fact, TA1 reduced the inherent alloresponse and actually enhanced HeLa cell proliferation. This was particularly apparent at the 25:1 ratio. This finding agrees with previous studies which have demonstrated that TA1 increases Treg cells and reduces Teff cells resulting in a decreased Th17:Treg ratio and a tolerogenic microenvironment.(Wang et al., 2011, 2015; Wang et al., 2012) To further characterize the active fraction of IA1, the anti-proliferative effects of resting PBMC pretreated with either the < 30 or ≥30 kDa fractions of IA1 were examined (Fig. 5E). As anticipated by Fig. 1, the cytokine-rich fraction (< 30 kDa) pretreated PBMC showed no significant variation from resting PBMC (dotted blue line). In contrast, the miRNA-containing ≥30 kDa fraction of IA1 mediated the anti-HeLa effects and was almost indistinguishable from the complete IA1 preparation (dotted red line) at the 50:1 ratio.

Purified PBMC consist of lymphocytes (T cells, B cells, NK cells) and monocytes. It is possible that IA1 could directly interact with each of these subsets and enhance their anti-cancer efficacy. To better elucidate

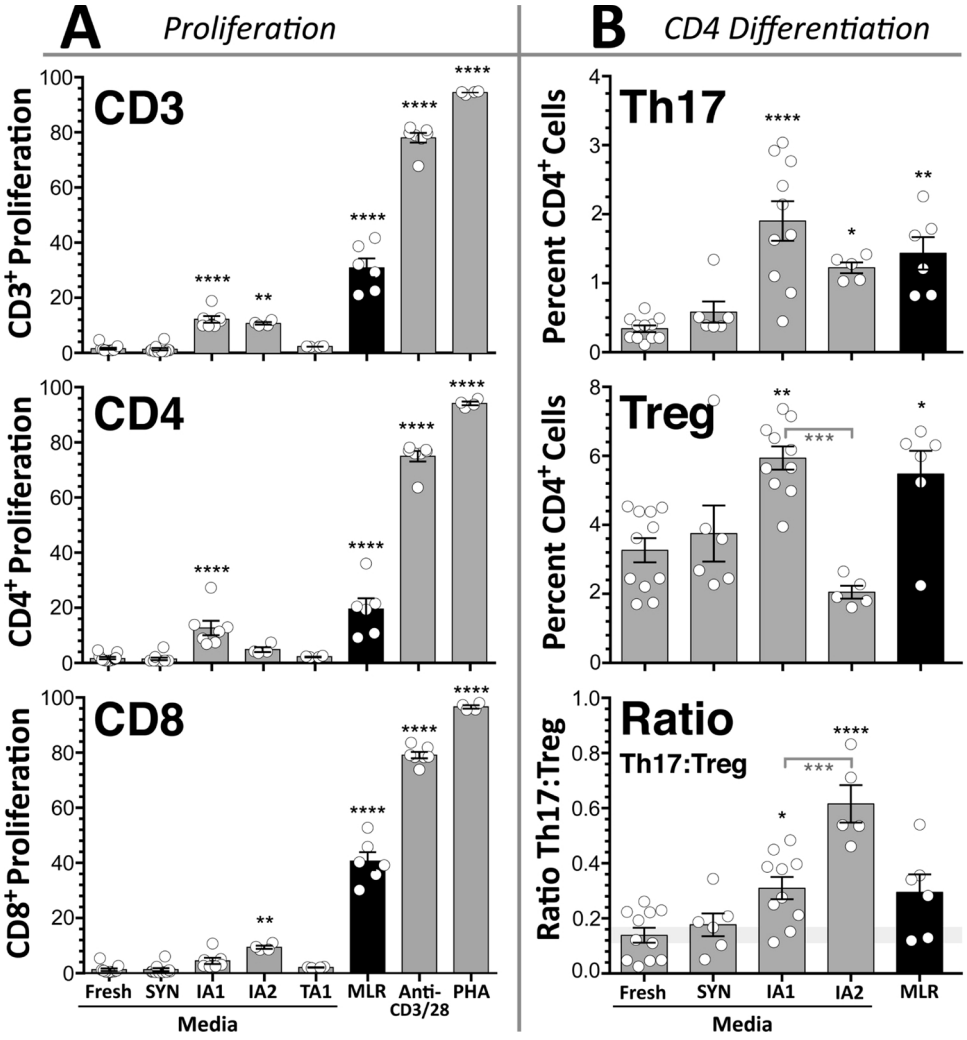

Fig. 3. IA1 and IA2 promoted differential subset proliferation of resting PBMC and in a significantly more restrained manner than pan T cell activators. **Panel A:** Shown are the proliferation of resting $CD3^+$, $CD4^+$ and $CD8^+$ (top to bottom, respectively) human T lymphocytes. Resting CFSE labeled PBMC were treated with Fresh, SYN, IA1, IA2 or TA1 for 10 days. The acellular secretome preparations were added 1:1 into AIM V growth media. Shown for comparison are the proliferative response of a control allogeneic MLR (black bar) and treatment of the same PBMC (as the secretome samples) with the pan-T cell activators anti-CD3/anti-CD28 and PHA. Data for the MLR, anti-CD3/anti-CD28 and PHA were collected at days 10, 3 and 4 respectively. $CD3^+$, $CD4^+$ and $CD8^+$ T lymphocyte subset proliferation was determined *via* flow cytometry. **Panel B:** The pro-inflammatory state (*i.e.*, ratio of Th17:Treg)was determined for the Fresh, SYN, IA1, IA2 and MLR (black bar) at day 10. The Th17:Treg (*i.e.*, Teff:Treg) ratio of PBMC incubated in fresh media (grey shaded areas) is indicated as is the mean ± SEM. Significance was calculated in comparison to fresh unless otherwise specified and denoted as: * $p < 0.05$; ** $p < 0.01$; *** $p < 0.001$; and **** $p < 0.0001$. N ≥ 4 for all samples.

the effect of IA1 on T cells within the PBMC, $CD4^+$ and $CD8^+$ subset purification studies were done (Fig. 5**F-H**). This was of interest as studies of IA1 on resting PBMC (Fig. 3) suggested a critical role for $CD4^+$ T cells while in an allorecognition (MLR; Fig. 4) model $CD8^+$ T cells were implicated. As shown in Fig. 5F, alloresponsive resting $CD8^+$ T lymphocytes accounted for the loss of HeLa cell proliferation; indeed, resting $CD4^+$ T cells demonstrated no alloresponsive, nor anti-cancer, effect and completely failed to inhibit HeLa cell proliferation. In contrast, when $CD4^+$ T cells were pretreated (24 h) with IA1 or IA2, these cells demonstrated significant anti-HeLa effects (Fig. 5G). The anti-HeLa effect was most pronounced with IA1 (as was anticipated by Fig. 3). Similarly, IA1 greatly enhanced the anti-HeLa efficacy of $CD8^+$ T cells (Fig. 5H). In contrast, IA2-activated $CD8^+$ T cells had minimal effect on HeLa cell proliferation. This finding was somewhat surprising as IA2 treatment of resting PBMC (in the absence of HeLa cells) increased $CD8^+$, relative to $CD4^+$, T cell proliferation (Fig. 3). Contrary to IA1 and IA2, SYN treated $CD4^+$ or $CD8^+$ subsets (**Panels G-H**) were no more effective than resting cell subsets (**Panel F**) at inhibiting HeLa growth. Of note, neither IA1 or IA2 pretreated purified $CD4^+$ or $CD8^+$ T cells inhibited HeLa cell proliferation as effectively as unfractionated PBMC (Fig. 5**C-D**); likely consequent to the well described synergistic interaction of $CD4^+$ and CD8 + T cells and, potentially, a small additive effect of monocytic cells found within the PBMC in cancer cell killing.(Haabeth et al., 2014; Hadrup et al., 2013)

A key component of T cell mediated inhibition of cancer cell proliferation is the direct interaction of the immune cell with the target cell. To investigate the interactions between control and IA1/IA2-activated PBMC with HeLa cells, time-lapse video microscopy and cell conjugation studies were conducted. As illustrated in Fig. 6A, IA1 and IA2 treated PBMC exhibited significantly greater interaction with HeLa cells than did resting PBMC. Microscopically, this was most pronounced with IA1, *versus* IA2, as noted by the greater degree of clustering of PBMC (white arrows) and individual HeLa cells (asterisk). Interestingly, the IA2-PBMC treated HeLa cells (black open arrows) demonstrated significant cellular vesiculating/blebbing and morphology alterations not observed in the IA1-PBMC sample. These morphological changes may be characteristic of IA2 associated apoptosis/necrosis. These microscopic cell:cell observations were further confirmed using a cell:cell conjugation assay (Fig. 6B). As noted, both IA1 and IA2 significantly increased PBMC:HeLa conjugation while the SYN media had no effect. Consequent to the enhanced cell:cell (PBMC:HeLa) interactions, HeLa cell proliferation was significantly decreased in the IA1 and IA2, but not SYN, treatment groups (Fig. 6C). Hence, both IA1 and IA2 activated resting PBMC exerted a potent anti-HeLa effect.

To further assess the anti-cancer utility of IA1 and IA2, the highly metastatic SH-4 melanoma cell line was examined. Interestingly, as shown in Fig. 7A, in the absence of any PBMC, both IA1 and IA2 directly inhibited SH-4 proliferation. The direct anti-proliferative effect was most apparent for IA2, and similar to that seen with HeLa cells, suggesting that IA2's direct mechanism of action could be broad spectrum. However, despite IA1's lack of direct toxicity on HeLa cells, IA1 significantly inhibited SH-4 proliferation; though the SH-4 cells did demonstrate a slow but consistent proliferation over time (Fig. 7A). As shown in Fig. 7**B-C**, resting PBMC at a 50:1 ratio exhibited an allo-/anti-

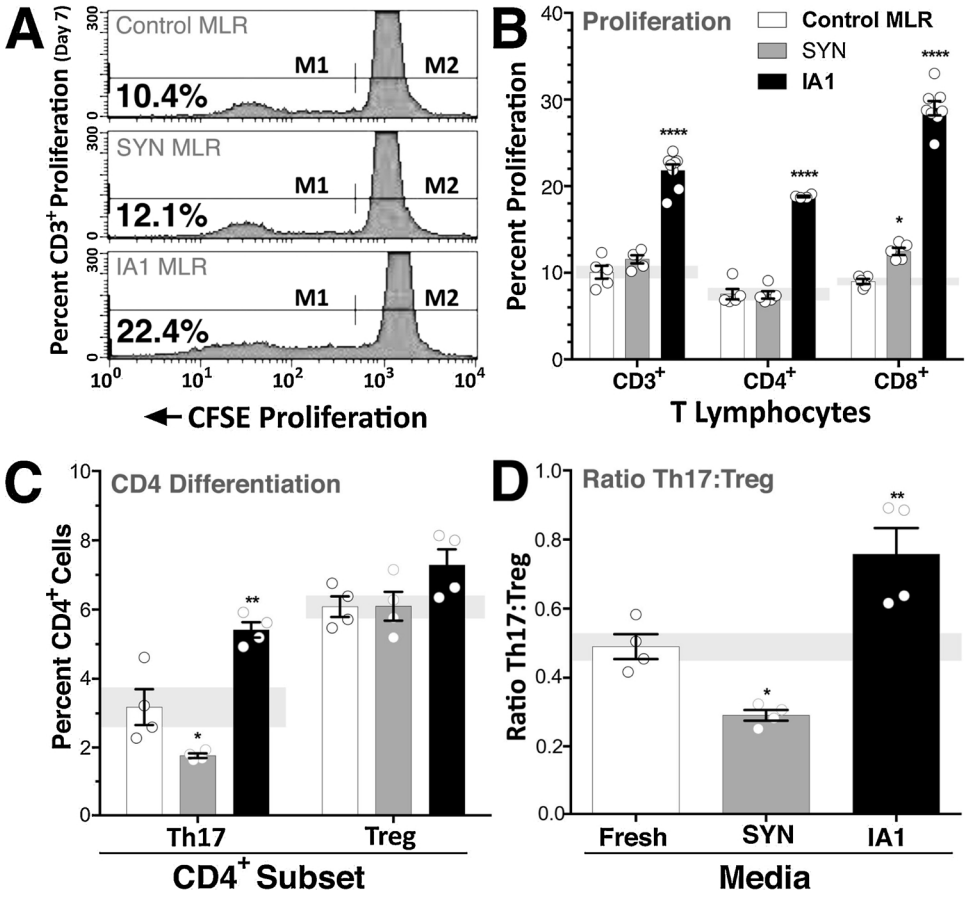

Fig. 4. IA1 accelerated the allorecognition pathway and significantly enhanced the alloproliferative response of the MLR. **Panel A:** Representative histograms of MLR T lymphocyte proliferation. M1 demonstrated the CFSE dilution upon cell proliferation while M2 indicated the non-proliferative population. **Panel B:** IA1, but not SYN, significantly enhanced the proliferation of $CD3^+$, $CD4^+$ and $CD8^+$ human T lymphocytes within a MLR alloproliferation model. **Panel C:** Flow cytometric studies demonstrated that IA1 significantly upregulated Th17 $CD4^+$ T cells while having minimal effects on Treg cells. **Panel D:** Consequent to the IA1-mediated increase in Th17 cells, the pro-inflammatory state (Th17:Treg) was significantly enhanced relative to the control (Fresh) MLR. Each acellular preparation was added 1:1 into AIM V growth media. Grey shaded horizontal bar (**Panels B-D**) areas represent the control (*i.e.*, Fresh; mean ± SEM) MLR values for comparative purposes. Values shown are the mean ± SEM for Day 7. Significance is denoted as: * $p < 0.05$; ** $p < 0.01$; *** $p < 0.001$; and **** $p < 0.0001$. N ≥ 4 for all samples.

cancer response resulting in the loss of SH-4 proliferation and cell death starting after approximately 72 h. Importantly, both IA1 and IA2 pretreatment of same donor resting PBMC (Fig. 7**B** and **C**, respectively) enhanced their anti-proliferative effects on SH-4 cells; though IA1 was significantly superior to IA2. The potency of IA1-activated PBMC was readily apparent even at a very low 10:1 ratio and was even more dramatic at increased PBMC numbers (**Panel B**). Indeed, with IA1 activation at both the 25:1 and 50:1 ratio, minimal SH-4 proliferation was noted over the first 48 h and the SH-4 cell death (*i.e.*, decreased impedance) became readily apparent by 48 h. IA2-activation also enhanced PBMC-mediated SH-4 inhibition but to a much lesser degree and required a longer time (≥ 72 h) until cell killing (decrease in cell impedance) was obvious. The results of IA1 and IA2 (both direct toxicity and PBMC activation) suggested that IA1 and IA2 were not equivalent and functioned, at least partially, *via* different mechanisms.

Immune cell activation occurs consequent to a number of factors including altered intracellular miRNA expression in response to immunomodulatory agents. (Carissimi et al., 2014; Thiele et al., 2012; Curtale et al., 2010) Indeed, miRNA are key regulators of cellular differentiation and proliferation and can serve as highly sensitive biomarkers of immune activation, tolerance, or quiescence. (Alvarez-Garcia and Miska, 2005; Jeker and Bluestone, 2013; Dooley et al., 2013) To examine the effect of the IA1 and IA2 secretome preparations on subsequent intracellular miRNA expression, resting PBMC were examined. As shown in Fig. 8**A**, clustergram expression profiles of resting PBMC incubated for 72 h in fresh and SYN media were similar across the majority of the 84 miRNA examined. Similarly, the tolerogenic TA1 therapeutic was also very closely aligned to resting cells in the fresh media despite being generated in an mPEG-MLR system biologically capable of allorecognition (blocked only by the membrane grafted polymer). In contrast, both IA1 and IA2 demonstrated significant variances from the profile of the control PBMC (**Fig.B**). Moreover, as indicated by the yellow boxes in **Fig.B**, IA1 and IA2 were very dissimilar to each other over a broad range of miRNA demonstrating that the induced T cell activation pathways were not equivalent (**IA1 ≠ IA2**) as anticipated by the findings shown in Figs. 3 and 5–7. As can be observed, the expression of numerous miRNA was vastly altered by IA1 treatment while IA2 treated PBMC more closely resembled the control sample. Interestingly, despite the disparities noted in miRNA expression of treated resting PBMC, IA1 and IA2 increased $CD3^+$ T cell proliferation to a similar level; however, a significant ($p < 0.05$) discrepancy of $CD4^+$ and $CD8^+$ T cell proliferation (Figs. 3 and 8**C**) was noticed as IA1 was $CD4^+$-centric while IA2 was $CD8^+$-centric. All these observations could contribute to the differential functions between IA1 and IA2. In contrast to the more restrained proliferation seen with IA1 and IA2, activation of resting PBMC using anti-CD3/anti-C28 or PHA resulted in distinctly divergent miRNA expression patterns to either IA1 or IA2; likely consequent to these agents near universal activation and proliferation of $CD3^+$ T cells (Fig. 3).

4. Discussion

The theory and practice of 'modern' pro-inflammatory (*i.e.,* increased Teff:Treg ratio) immunotherapy arguably originated in 1891 with William Coley's treatment of cancer patients with bacteria (and later other toxins) to induce an immune response that would exert a toxic bystander effect on a tumor mass.(Coley, 1891, 1910; Coley, 1913, 1893) Despite some clinical success, and their availability until 1962, Coley's Toxins garnered criticisms from within the medical community and were eventually supplanted by the newer, and *'safer'*, developments of radiation and chemo- therapy; which themselves pose significant short- and long-term risks to the patient.(Coley, 1891, 1910; Coley, 1913, 1893; Starnes, 1992) Today, almost 130 years later, immunotherapy has refocused on Coley's core principles of inducing the

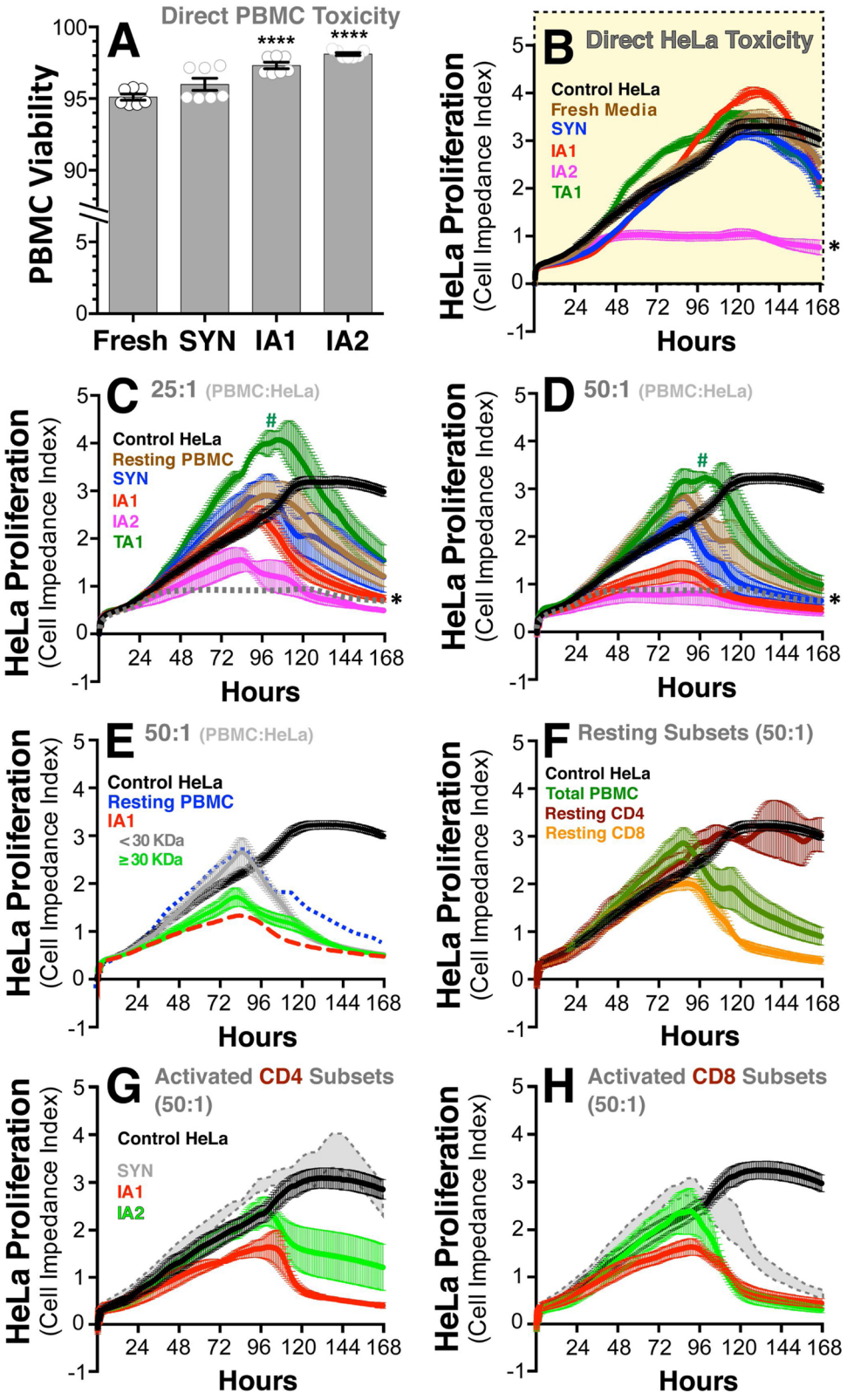

Fig. 5. HeLa cell cancer model. **Panel A:** Neither IA1 nor IA2 exerted any direct PBMC toxicity over the 24 h used for PBMC pretreatment as assessed at 24 h using 7 AAD. Shown are the mean ± SEM for a minimum of 3 independent experiments. **Panel B:** The direct HeLa cell toxicity of the SYN, IA1, IA2 and TA1 secretome products (ratio of 1:1 with HeLa growth media) was assessed. As shown, SYN, IA1 and TA1 had no effect on HeLa cell proliferation relative to the control sample. In contrast, IA2 exerted a potent and direct toxicity to HeLa cells. **Panels C-D:** Shown are HeLa cell growth curves when overlaid at a 25:1 or 50:1 ratio (Panels C and D, respectively) with resting PBMC, or the same donor PBMC pretreated (24 h) with SYN, IA1, IA2 or TA1 prior to overlay. The dotted line (indicated by *) represents to direct IA2 HeLa cell toxicity shown in Panel B. **Panel E:** Supporting the findings observed in Fig. 1B, PBMC pretreatment with the cytokine poor, miRNA-enriched, ≥30kDa fraction of IA1 resulted in a potent anti-HeLa effect. In contrast, pretreatment with the cytokine rich < 30 kDa fraction of IA1 was indistinguishable from the SYN preparation. **Panel F-H:** To assess the relative roles of $CD4^+$ and $CD8^+$ T cell subsets on HeLa cell proliferation, purified $CD4^+$ and $CD8^+$ T cells were pretreated (24 h) with Fresh, SYN, IA1 or IA2. As shown in **Panel F**, $CD8^+$ T cells solely conferred the anti-Hela effect observed with resting PBMC. In stark contrast, $CD4^+$ resting cells showed no anti-HeLa effects. However, pretreatment of purified $CD4^+$ T cells with IA1, and to a slightly lesser extent IA2, resulted in a potent anti-HeLa effect relative to the resting $CD4^+$ T cells or pretreatment with the SYN agent (**Panel G**). Additionally, IA1 (in particular) and IA2 greatly enhanced the anti-HeLa efficacy of $CD8^+$ T cells as well (**Panel H**). In Panels B–H cell proliferation was continuously monitored in real-time over 7 days as a function of the cell impedance index using an ACEA iCELLigence. The proliferation curves shown present the mean ± SEM of a minimum of 4 independent samples. HeLa cells were seeded at an initial density of 5000 cells per well. PBMC were pretreated with the indicated agent and then extensively washed prior to being overlaid onto the HeLa cells.

endogenous immune response. Ironically, similar to Coley's use of bacteria, genetically modified strains of *Salmonella* sp., as well as recombinant polioviruses, have been used to induce an inflammatory microenvironment at the tumor site.(Frahm et al., 2015; Zheng et al., 2017; Desjardins et al., 2018) Additionally, tumor-specific immunotherapy has been explored in which autologous cancer cells are isolated, modified, and re-infused into the patient in an attempt to enhance anti-cancer immune cell activation.(Schulof et al., 1988; Ockert et al., 1996; Baars et al., 2002; Berger et al., 2007; Fishman et al., 2008) More recently, autologous or allogenic adoptive cell transfer (ACT) immunotherapy, especially CAR-T cell therapy, have become important clinical tools.(Bach et al., 2017; D'Aloia et al., 2018; Mullard, 2017) However, while ACT, and CAR-T cells in particular, will prove to be a crucial tools in cancer immunotherapy, they are

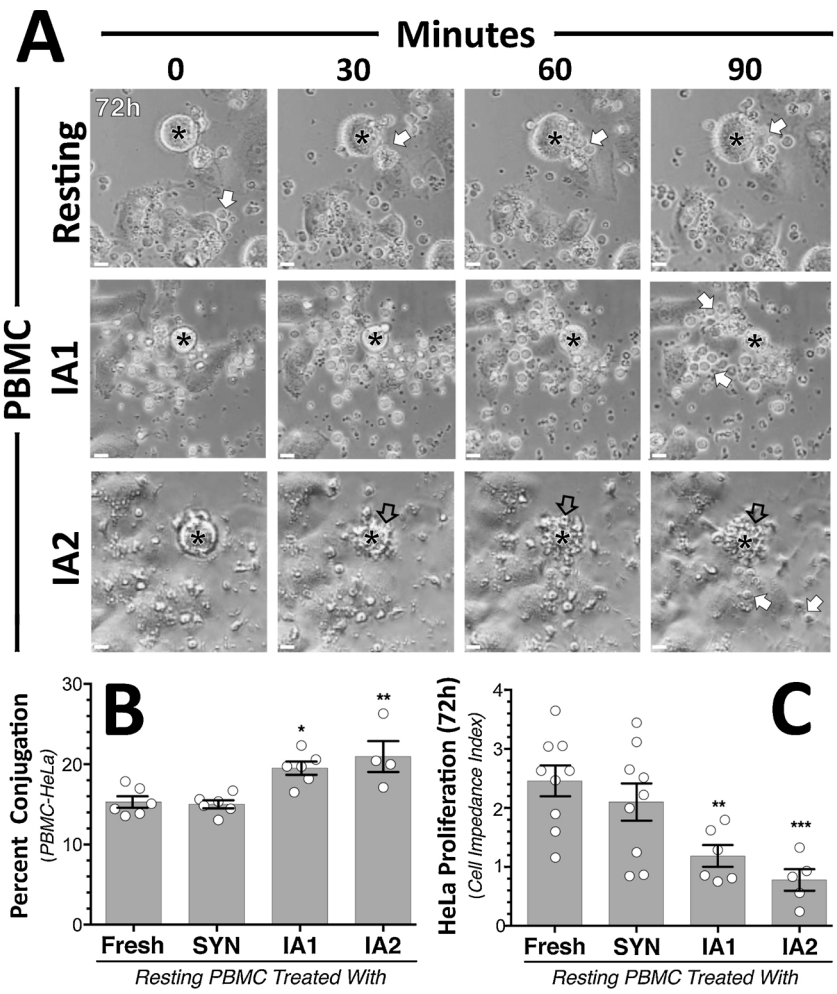

Fig. 6. IA1 and IA2 differentially affected PBMC-HeLa cell interactions as shown by photomicroscopy and cell conjugation assays. Findings shown were obtained using a PBMC:HeLa ratio of 50:1. **Panel A:** Representative images of PBMC-HeLa conjugation shot at 0, 30, 60 and 90 min during the time-lapse video. The black asterisks indicated representative HeLa cells, the white arrows pointed at PBMC. Black open arrows demonstrated blebbing of HeLa cells. Time-lapse video was acquired for 90 min after 72 h of PBMC and HeLa cell co-culture. Images shown are representative frames at the indicated times from one of three independent experiments. Size bar = 10 μm. **Panel B:** IA1 and IA2 significantly enhanced conjugation between CFSE labeled PBMC and Far-Red labeled HeLa cells after 20 min' co-culture as measured by flow cytometry. **Panel C:** HeLa cell proliferation index at 72 h (derived from Fig. 5C) post overlay with IA1 or IA2 pretreated PBMC correlated with the microscopic and flow cytometric findings. **Panels B-C:** Shown are the mean ± SEM. The individual experiments are shown with the white circles with a minimum of 5 independent experiments for each condition. Significance was calculated in comparison to fresh unless otherwise specified and denoted as: * $p < 0.05$; ** $p < 0.01$; *** $p < 0.001$; and **** $p < 0.0001$. For all samples N ≥ 4.

accompanied by significant issues including cost, manufacturing time (weeks-months) and safety (*e.g.*, cytokine release syndrome induction). (Bonifant et al., 2016; Bach et al., 2017; Lesterhuis et al., 2011; Perica et al., 2015) But are there other, safer, faster, and lower-cost ACT-immunomodulatory approaches that could be used to stimulate a patient's autologous immune response?

As evidenced in this study, and previous publications, the secretome of immunological cells can be used to exert potent immunomodulatory effects both *in vitro* and *in vivo*.(Kang et al., 2017; Wang et al., 2011, 2015) Importantly, the biomanufacturing conditions dictate the secretome generated allowing for the reproducible production of either tolerogenic or pro-inflammatory agents. Indeed, a previous study from our laboratory demonstrated that a tolerogenic miRNA–Based secretome (TA1; Figs. 1 and 3) could enhance the production of Treg cells

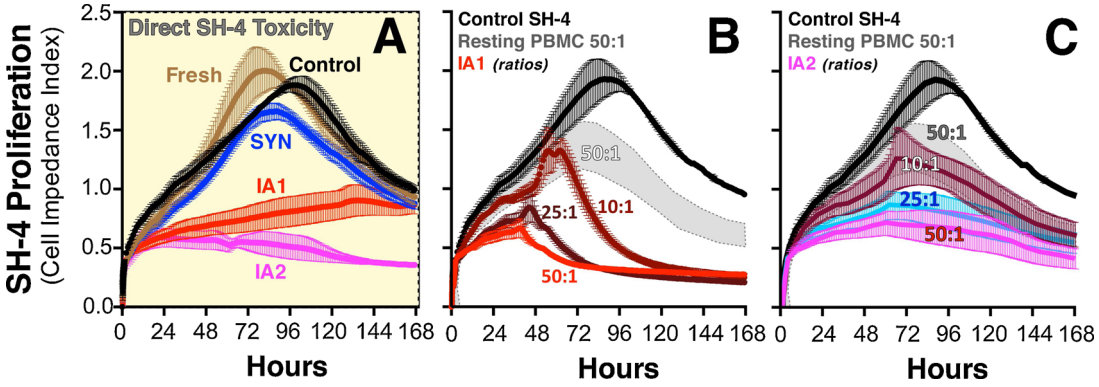

Fig. 7. IA1 and IA2 attenuated SH-4 cell proliferation *via* both direct SH-4 toxicity as well as enhancing PBMC-mediated growth inhibition. **Panel A:** In contrast to HeLa cells, both IA1 and IA2 demonstrated direct toxicity/growth arrest to SH-4 cells. The SYN product had minimal inhibitory effect on SH-4 proliferation. **Panel B:** IA1 pretreatment of resting PBMC significantly increased their inhibition of SH-4 proliferation. Shown are the effects of IA1-activated PBMC (red lines) at ratios to SH-4 cells of 10:1, 25:1 and 50:1 relative to SYN-treated PBMC at a ratio of 50:1 (shaded area). Indeed, SH-4 proliferation was significantly inhibited by IA1-activated PBMC within a few hours of overlay. **Panel C:** IA2-activated PBMC (10:1, 25:1 and 50:1 ratios) also inhibited SH-4 cell proliferation though to a much lesser extent than IA1. Proliferation curves shown represent mean ± SEM of a minimum of three independent experiments (For interpretation of the references to colour in this figure legend, the reader is referred to the web version of this article).

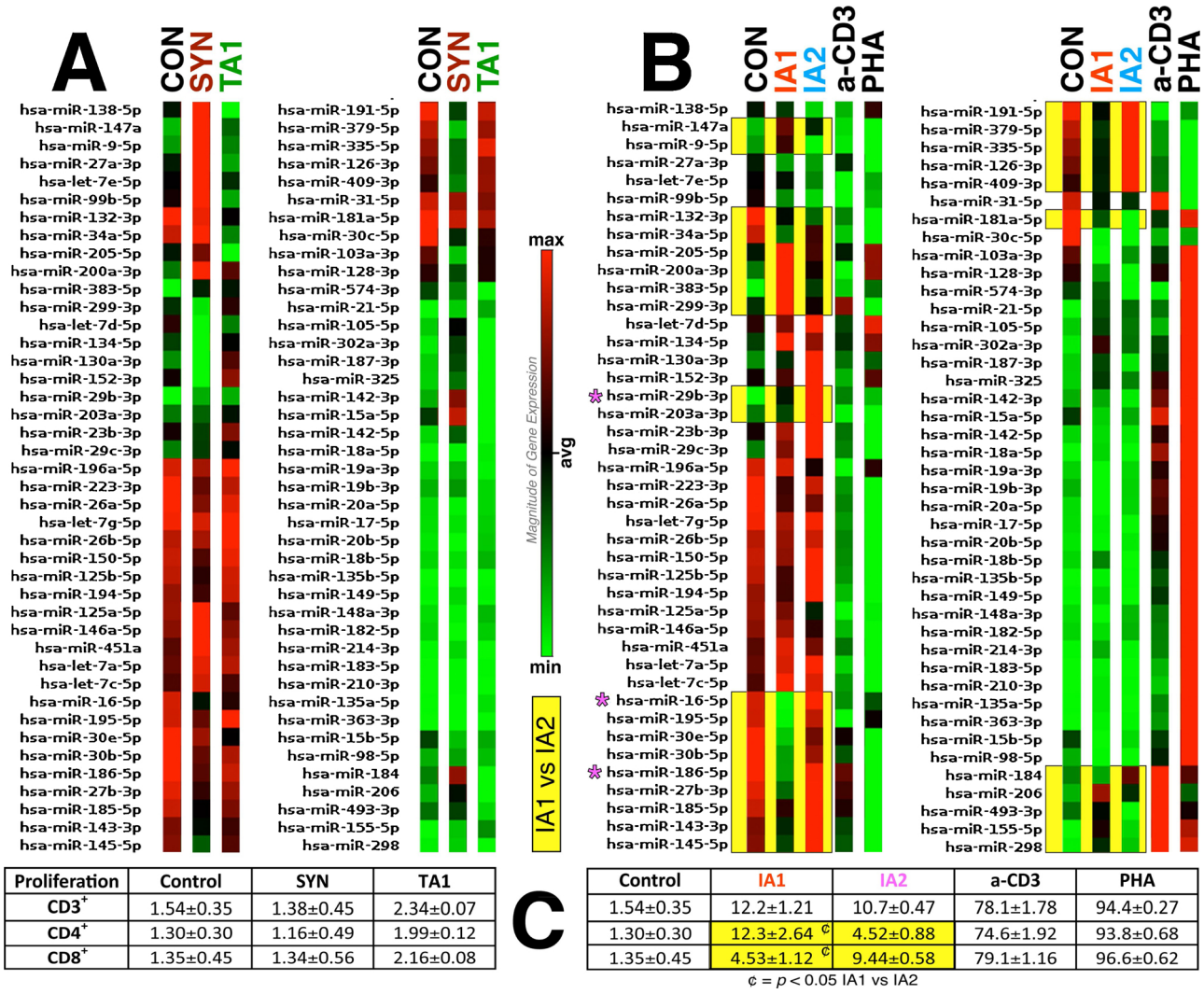

Proliferation	Control	SYN	TA1
CD3$^+$	1.54±0.35	1.38±0.45	2.34±0.07
CD4$^+$	1.30±0.30	1.16±0.49	1.99±0.12
CD8$^+$	1.35±0.45	1.34±0.56	2.16±0.08

Control	IA1	IA2	a-CD3	PHA
1.54±0.35	12.2±1.21	10.7±0.47	78.1±1.78	94.4±0.27
1.30±0.30	12.3±2.64 ¢	4.52±0.88	74.6±1.92	93.8±0.68
1.35±0.45	4.53±1.12 ¢	9.44±0.58	79.1±1.16	96.6±0.62

¢ = $p < 0.05$ IA1 vs IA2

Fig. 8. IA1 and IA2 pretreatment induced differential intracellular miRNA expression profiles in resting PBMC. To partially assess the effect of the secretome-derived products on PBMC, miRNA arrays were conducted on resting, SYN, IA1, IA2, anti-CD3/anti-CD28 and PHA stimulated PBMC at 72 h post-treatment. Total RNAs were extracted from treated cells for the profiling of 84 miRNA differentially expressed during normal and pathological immune responses. **Panel A:** miRNA clustergram expression profiles of PBMC treated with SYN and TA1 in comparison to Control. **Panel B:** miRNA expression profiles of PBMC treated with IA1, IA2, anti-CD3/anti-CD28 or PHA in comparison to Control. Yellow boxed indicated differential miRNA patterns between IA1 and IA2 treatment. Yellow (*) represented pro-apoptotic miRNA differentially upregulated in IA2 relative to IA1. Clustergram data in A–B represent three independent experiments. **Panel C:** Proliferation rates of CD3$^+$, CD4$^+$ and CD8$^+$ T cells in the indicated conditions (derived from Fig. 3). Shown are the mean ± SEM of a minimum of 4 independent experiments. ¢ $p < 0.05$. (For interpretation of the references to colour in this figure legend, the reader is referred to the web version of this article).

(and simultaenosuly decrease Teff cells) and effectively inhibit the onset of Type 1 diabetes in NOD mice.(Kang et al., 2017; Wang et al., 2011, 2015) Moreover, as demonstrated in the current report, the allorecognition-based acellular IA1 secretome preparation can be used as a pro-inflammatory adjuvant for autologous ACT therapy by enhancing the proliferative response of resting lymphocytes and increasing the Teff:Treg ratio and thereby increasing PBMC anti-cancer activity.

Of note, despite IA1 being biomanufactured from the secretome of the allorecognition response, IA1 activated lymphocytes are not MHC-restricted and the acellular IA1 therapeutic poses no risk of GvHD. Efficacy of IA1 is mediated by a complex mixture of soluble and exosome-encapsulated miRNA arising from the MLR allorecognition microenvironment; not residual cytokines within the IA1 preparation (Fig. 1). The use of a bioreactor system to produce the therapeutic miRNA was critical due to the complexity and low fidelity of miRNA bioregulatory pathways. Based on the complicated regulatory action of miRNA, we consciously chose an anti-reductionist approach to produce a ***complex pattern of miRNA expression*** that mimics normal biology in order to achieve maximal biological functionality. In biology, it is important to note that activation of some, and inhibition of other, pathways interplay to produce a biological response to stimuli. Thus, a pattern of expression, comprising both INCREASED and DECREASED miRNA species, is essential for effective immunomodulation of the recipient – making the miRNA cocktail similar to therapeutic intravenous immunoglobulin (IVIG) which consists of hundreds of thousands of unique IgGs from thousands of donors. Due to the evolutionary conservation of miRNA, and the miRNA bioregulatory process, significant cross-species (human ↔ mouse) efficacy was noted with the IA1 biotherapeutic (Fig. 2).

Importantly, the secretome produced IA1 exerted no *ex vivo* toxicity to PBMC (Fig. 5A), or primary cells, making the product suitable for autologous ACT therapy. IA1 did, however, induce a significant pro-inflammatory response within resting T lymphocytes (Figs. 1–3), increase the Teff:Treg ratio (Figs. 1–3) and enhance an existing immune response (MLR; Fig. 4); effects that would be beneficial in individuals with absent or weak endogenous anti-cancer responses. The enhancement of an endogenous response can also be observed in our cancer cell line models which employed allogenic PBMC. As noted in Figs. 5–7

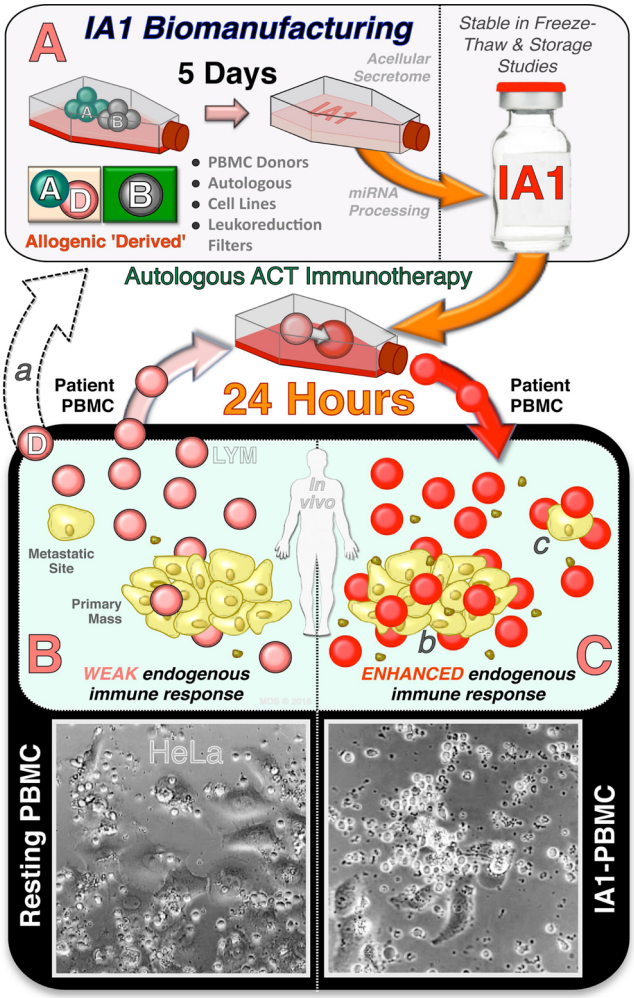

Fig. 9. Schematic presentation of use and mechanism of action for IA1 secretome therapeutic. **Panel A:** Bioreactor production of IA1 secretome is readily accomplished using an allogenic MLR. Source materials include PBMC donors (A and B), autologous cells (*a*; as one donor), lymphocytic cell lines, or leukoreduction filters from blood collection bags. Acellular supernatant is collected at day 5 for processing into IA1 (Fig. 1). IA1 is stable for months when aliquoted and frozen. **Panels B-C:** Weak to absent immune response to both the primary tumor and metastatic sites allows for cancer progression. PBMC (D) from the patient are treated *ex vivo* for 24 h with IA1 and then reinfused into the individual where they show enhanced recognition and killing of the primary tumor (*b*) and, potentially, improved immune surveillance at metastatic sites (*c*). This is supported by photomicrographs of allogenic PBMC responding to HeLa cells. As shown, after 72 h incubation, resting (weak responders; *left*) PBMC show limited interaction when overlaid on HeLa cells. In contrast, the same PBMC, when treated for 24 h with IA1, show a robust enhanced interaction (*right*) with the HeLa cell monolayer.

resting PBMC would, after ˜4–5 days of co-culture, inhibit and eventually kill the HeLa cells; likely due to both allogenic and anti-cancer responses. However, the anti-proliferative response was vastly accelerated (*i.e.,* pre-primed) and enhanced by treating the resting PBMC for 24 h with IA1 prior to overlaying onto the cancer cells. Importantly, IA1 induced a significantly more restrained proliferative response than either mAb (*e.g.,* anti-CD/anti-CD28) or mitogen (*e.g.*, PHA) induced activation of resting PBMC. Indeed, the clustergram analysis of IA1 (or IA2) on miRNA expression of treated cells was dramatically different than, and often inverse to, that of the anti-CD3/anti-CD28 or PHA stimulated cells (Fig. 8).

How could IA1 be utilized in ACT therapy? As diagrammatically shown in Fig. 9, the bioproduction of IA1 (and IA2) from the secretome is both inexpensive and rapid (5 days) and the IA1 can be stored for long periods (several months frozen in the laboratory; data not shown). Moreover, neither IA1 (nor IA2) production actually requires tissues (PBMC or, for IA2, cancer cells) derived from the patient making it an *'off-the-shelf'* immune adjuvant. Most importantly for patient care, *ex vivo* activation of lymphocytes is rapid (24 h); in stark contrast to the weeks to months necessary for production and expansion of CAR-T cells. The IA1-activated cells exhibited dramatically enhanced immune recognition of cancer cells over resting PBMC as evidence in photomicrographs and proliferation assays (Fig. 9**B-C**). Hence, IA1 activation of autologous PBMC could employed as a first line therapy or, potentially, be used in an immunotherapeutic bridge while CAR-T cells are produced. Due to the simplicity and low cost of the approach, multiple rounds could be used as necessary with large numbers of autologous PBMC employed. Indeed, due to the ability to infuse large numbers of IA1 treated autologous cells, enhanced recognition of not only the primary tumor but metastatic sites as well could be achieved thus improving long-term survival. Of note, similarly to our previous study on the tolerogeneic TA1 (Figs. 1**A and** 3 **A**) in the inhibition of Type 1 diabetes in NOD mice, IA1 or IA2 could be directly injected into the recipient yielding a systemic reset of the immune system.(Wang et al., 2015)

Finally, in an attempt to determine if the anti-cancer efficacy of the alloresponse-based IA1 could be improved upon, the anti-HeLa acellular secretome product IA2 was similarly studied. Somewhat surprisingly, despite the broad similarity in the bioproduction of IA1 and IA2 (Fig. 1A), the resultant secretome-based agents exhibited significant immunological and anti-cancer differences. As noted in Fig. 5, IA2-treated PBMC were more effective at inhibiting HeLa cell proliferation than were the same PBMC pretreated with IA1 – suggesting a HeLa cell specificity. Indeed, this observation was supported by the finding that IA2-treated PBMC were less effective than IA1-treated PBMC in inhibiting SH-4 proliferation (Fig. 7). At the T cell level, upon stimulation of resting $CD3^+$ T lymphocytes, IA1 predominantly increased $CD4^+$ while IA2 predominantly increased $CD8^+$ T cell proliferation. Among $CD4^+$ subsets, both IA1 and IA2 expanded the Th17 subset but IA2 simultaneously shrank the Treg resulting in a larger magnitude of increase in the Th17:Treg ratio in the IA2 treated PBMC. Intriguingly, despite the enhanced killing of HeLa cells by the IA2 treated PBMC, purified $CD4^+$ or $CD8^+$ T cell subpopulations treated with IA2 were not as effective as the same subpopulations pre-treated with IA1 (Fig. 5). Evidence of these immunologic disparities may be seen in the inverse expression patterns of several miRNA noted in resting PBMC treated with IA1 *versus* IA2 suggesting differential activation pathways (Fig. 8).

More interestingly, the IA2 biotherapeutic demonstrated significant direct toxicity to not only HeLa cell (from which it was derived) but also SH-4 cells (Figs. 5–7). This direct toxicity was morphologically suggestive of IA2 induced apoptosis with significant blebbing observed in the HeLa cells (Fig. 6A). This observation was supported by the observation that in IA2, but not IA1, treated PBMC, upregulation of several miRNA (Fig. 8; *e.g.,* miR-29b-3p, miR-186-5p, and miR-16-5p) associated with apoptosis was apparent.(Singh and Saini, 2012; Pileczki et al., 2016; Zhou et al., 2010) Hence, IA1 ≠ IA2 suggesting that the cell types [lymphocyte:lymphocyte *versus* lymphocyte:epithelial (*i.e.,* HeLa)] utilized in the bioproduction alters the composition of the secretome and the derived miRNA-enriched product. This would not be surprising since cells produce and export free and exosome encapsulated miRNA, the composition of which will vary based on cell type, activation state and function.(Di Santo et al., 2009; Lee et al., 2015; Dowling and Clynes, 2011; Sholl-Franco and Araujo, 1997) Ongoing studies are investigating the differential effects of cell types on bioreactor produced secretomes and miRNA.

In sum, bioreactor production of the lymphocyte allorecognition secretome yields a miRNA–Based, MHC-independent, biotherapeutic (IA1) that can be reproducibly manufactured and exhibits potent immunomodulatory activity. The IA1 biotherapeutic is both easy and

inexpensive to produce and can be used *ex vivo* to induce a rapid (24 h of incubation) pro-inflammatory response in resting, patient sourced, autologous PBMC that may dramatically enhance their anti-cancer efficacy upon reinfusion into the donor. Furthermore, by altering the type of tissue (*e.g.*, cancer cell *versus* lymphocyte) to which the lymphocyte population is responding to, other secretome-biotherapeutics can be derived that may be capable of inducing apoptosis in targeted tissues. Successful development of this secretome biotherapeutic/manufacturing approach may prove useful in both treating cancer and in preventing/reducing the metastatic potential of existing cancers.

CONFLICT OF INTERESTS

All authors have read the journal's policy on disclosure of potential conflicts of interest. *Canadian Blood Services* is pursuing patents related to the production and utilization of the described acellular immunomodulatory agents. *Canadian Blood Services*, a not-for-profit organization responsible for collecting, manufacturing and distributing blood and blood products to all Canadians (except Quebec), is the assignee for relevant patents. MDS and WMT are inventors on these patents. XY and NK have no conflicts of interest beyond bring paid by *Canadian Blood Services*.

Acknowledgements

The authors would like to thank Dr. Duncheng Wang for his technical contributions to this study. This work was supported by grants from the Canadian Institutes of Health Research (Grant No. 123317; MDS), Canadian Blood Services (MDS) and Health Canada (MDS). The views expressed herein do not necessarily represent the view of the federal government of Canada. We thank the Canada Foundation (CFI) for Innovation and the Michael Smith Foundation for Health Research for infrastructure funding at the University of British Columbia Centre for Blood Research. The funders had no role in study design, data collection and analysis, decision to publish, or preparation of the manuscript.

References

Abul, K.A., Andrew, H.H.L., Shiv, P., 2015. Basic Immunology E-Book.
Alvarez-Garcia, I., Miska, E.A., 2005. MicroRNA functions in animal development and human disease. Development 132, 4653–4662.
Arroyo, J.D., Chevillet, J.R., Kroh, E.M., Ruf, I.K., Pritchard, C.C., Gibson, D.F., Mitchell, P.S., Bennett, C.F., Pogosova-Agadjanyan, E.L., Stirewalt, D.L., Tait, J.F., Tewari, M., 2011. Argonaute2 complexes carry a population of circulating microRNAs independent of vesicles in human plasma. Proc. Natl. Acad. Sci. U. S. A. 108, 5003–5008.
Baars, A., van Riel, J.M., Cuesta, M.A., Jaspars, E.H., Pinedo, H.M., van den Eertwegh, A.J., 2002. Metastasectomy and active specific immunotherapy for a large single melanoma metastasis. Hepatogastroenterology 49, 691–693.
Bach, P.B., Giralt, S.A., Saltz, L.B., 2017. FDA approval of tisagenlecleucel: promise and complexities of a $475 000 Cancer drug. JAMA 318, 1861–1862.
Barrett, A.J., 1997. Mechanisms of the graft-versus-leukemia reaction. Stem Cells 15, 248–258.
Barrett, J., Childs, R., 2000. The benefits of an alloresponse: graft-versus-tumor. J. Hematother. Stem Cell Res. 9, 347–354.
Beer, L., Zimmermann, M., Mitterbauer, A., Ellinger, A., Gruber, F., Narzt, M.S., Zellner, M., Gyöngyösi, M., Madlener, S., Simader, E., Gabriel, C., Mildner, M., Ankersmit, H.J., 2015. Analysis of the secretome of apoptotic peripheral blood mononuclear cells: impact of released proteins and exosomes for tissue regeneration. Sci. Rep. 5, 16662.
Beer, L., Mildner, M., Gyöngyösi, M., Ankersmit, H.J., 2016. Peripheral blood mononuclear cell secretome for tissue repair. Apoptosis 21, 1336–1353.
Berger, M., Kreutz, F.T., Horst, J.L., Baldi, A.C., Koff, W.J., 2007. Phase I study with an autologous tumor cell vaccine for locally advanced or metastatic prostate cancer. J. Pharm. Pharm. Sci. 10, 144–152.
Bian, G., Ding, X., Leigh, N.D., Tang, Y., Capitano, M.L., Qiu, J., McCarthy, P.L., Liu, H., Cao, X., 2013. Granzyme B-mediated damage of CD8+ T cells impairs graft-versus-tumor effect. J. Immunol. 190, 1341–1350.
Bonifant, C.L., Jackson, H.J., Brentjens, R.J., Curran, K.J., 2016. Toxicity and management in CAR T-cell therapy. Mol. Ther. Oncolytics 3, 16011.
Cantrell, D.A., 2002. T-cell antigen receptor signal transduction. Immunology 105, 369–374.
Carissimi, C., Carucci, N., Colombo, T., Piconese, S., Azzalin, G., Cipolletta, E., Citarella, F., Barnaba, V., Macino, G., 2014. Fulci V. miR-21 is a negative modulator of T-cell activation. Biochimie 107 (Pt B), 319–326.
Coley II., W.B., 1891. Contribution to the knowledge of sarcoma. Ann. Surg. 14, 199–220.
Coley, W.B., 1893. The treatment of malignant tumors by repeated inoculations of erysipelas. With a report of ten original cases. Clin. Orthop. Relat. Res 19913-11.
Coley, W.B., 1910. The treatment of inoperable sarcoma by bacterial toxins (the mixed toxins of the Streptococcus erysipelas and the Bacillus prodigiosus). Proc. R. Soc. Med. 3, 1–48.
Coley IX, W.B., 1913. Contribution to the study of sarcoma of the femur: periosteal round-celled sarcoma of the femur, involving two-thirds of the shaft, with very extensive multiple metastases-apparent cure by the mixed toxins of Erysipelas and Bacillus prodigiosus. Well 10(1/2) years, when a malignant tumor (Sarcoma and Epithelioma) developed in the thigh at the site of an old X-Ray dermatitis. Ann. Surg. 58, 97–108.
Curtale, G., Citarella, F., Carissimi, C., Goldoni, M., Carucci, N., Fulci, V., Franceschini, D., Meloni, F., Barnaba, V., Macino, G., 2010. An emerging player in the adaptive immune response: microRNA-146a is a modulator of IL-2 expression and activation-induced cell death in T lymphocytes. Blood 115, 265–273.
D'Aloia, M.M., Zizzari, I.G., Sacchetti, B., Pierelli, L., Alimandi, M., 2018. CAR-T cells: the long and winding road to solid tumors. Cell Death Dis. 9, 282.
Desjardins, A., Gromeier, M., Herndon, J.E., Beaubier, N., Bolognesi, D.P., Friedman, A.H., Friedman, H.S., McSherry, F., Muscat, A.M., Nair, S., Peters, K.B., Randazzo, D., Sampson, J.H., Vlahovic, G., Harrison, W.T., McLendon, R.E., Ashley, D., Bigner, D.D., 2018. Recurrent glioblastoma treated with recombinant poliovirus. N. Engl. J. Med. 379 (2), 150–161.
Di Santo, S., Yang, Z., Wyler von Ballmoos, M., Voelzmann, J., Diehm, N., Baumgartner, I., Kalka, C., 2009. Novel cell-free strategy for therapeutic angiogenesis in vitro generated conditioned medium can replace progenitor cell transplantation. PLoS One 4, e5643.
Dooley, J., Linterman, M.A., Liston, A., 2013. MicroRNA regulation of T-cell development. Immunol. Rev. 253, 53–64.
Dowling, P., Clynes, M., 2011. Conditioned media from cell lines: a complementary model to clinical specimens for the discovery of disease-specific biomarkers. Proteomics. 11, 794–804.
Dunn, G.P., Koebel, C.M., Schreiber, R.D., 2006. Interferons, immunity and cancer immunoediting. Nat. Rev. Immunol. 6, 836–848.
Eljaafari, A., Van Snick, J., Voisin, A., Cormont, F., Farre, A., Bienvenu, J., Bernaud, J., Rigal, D., Thomas, X., 2006. Alloreaction increases or restores CD40, CD54, and/or HLA molecule expression in acute myelogenous leukemia blasts, through secretion of inflammatory cytokines: dominant role for TNFbeta, in concert with IFNgamma. Leukemia 20, 1992–2001.
Fabre, J.W., 2001. The allogeneic response and tumor immunity. Nat. Med. 7, 649–652.
Fishman, M., Hunter, T.B., Soliman, H., Thompson, P., Dunn, M., Smilee, R., Farmelo, M.J., Noyes, D.R., Mahany, J.J., Lee, J.H., Cantor, A., Messina, J., Seigne, J., Pow-Sang, J., Janssen, W., Antonia, S.J., 2008. Phase II trial of B7-1 (CD-86) transduced, cultured autologous tumor cell vaccine plus subcutaneous interleukin-2 for treatment of stage IV renal cell carcinoma. J. Immunother. 31, 72–80.
Frahm, M., Felgner, S., Kocijancic, D., Rohde, M., Hensel, M., Curtiss, R., Erhardt, M., Weiss, S., 2015. Efficiency of conditionally attenuated Salmonella enterica serovar Typhimurium in bacterium-mediated tumor therapy. MBio 6.
Gascoigne, K.E., Taylor, S.S., 2009. How do anti-mitotic drugs kill cancer cells. J. Cell. Sci. 122, 2579–2585.
Haabeth, O.A., Tveita, A.A., Fauskanger, M., Schjesvold, F., Lorvik, K.B., Hofgaard, P.O., Omholt, H., Munthe, L.A., Dembic, Z., Corthay, A., Bogen, B., 2014. How do CD4(+) t cells detect and eliminate tumor cells that either lack or express MHC class II molecules. Front. Immunol. 5, 174.
Hadrup, S., Donia, M., Thor Straten, P., 2013. Effector CD4 and CD8 T cells and their role in the tumor microenvironment. Cancer Microenviron. 6, 123–133.
Haider, T., Höftberger, R., Rüger, B., Mildner, M., Blumer, R., Mitterbauer, A., Buchacher, T., Sherif, C., Altmann, P., Redl, H., Gabriel, C., Gyöngyösi, M., Fischer, M.B., Lubec, G., Ankersmit, H.J., 2015. The secretome of apoptotic human peripheral blood mononuclear cells attenuates secondary damage following spinal cord injury in rats. Exp. Neurol. 267, 230–242.
Han, T., Takita, H., 1972. Immunologic impairment in bronchogenic carcinoma: a study of lymphocyte response to phytohemagglutinin. Cancer 30, 616–620.
Jeker, L.T., Bluestone, J.A., 2013. MicroRNA regulation of T-cell differentiation and function. Immunol. Rev. 253, 65–81.
Kang, N., Toyofuku, W.M., Yang, X., Scott, M.D., 2017. Inhibition of allogeneic cytotoxic T cell (CD8+) proliferation via polymer-induced Treg (CD4+) cells. Acta Biomater.
Kasiske, B.L., Snyder, J.J., Gilbertson, D.T., Wang, C., 2004. Cancer after kidney transplantation in the United States. Am. J. Transplant. 4, 905–913.
Kyluik-Price, D.L., Scott, M.D., 2016. Effects of methoxypoly (Ethylene glycol) mediated immunocamouflage on leukocyte surface marker detection, cell conjugation, activation and alloproliferation. Biomaterials 74, 167–177.
Kyluik-Price, D.L., Li, L., Scott, M.D., 2014. Comparative efficacy of blood cell immunocamouflage by membrane grafting of methoxypoly(ethylene glycol) and polyethyloxazoline. Biomaterials 35, 412–422.
Larsson, E.L., Coutinho, A., 1979. The role of mitogenic lectins in T-cell triggering. Nature 280, 239–241.
Le, Y., Scott, M.D., 2010. Immunocamouflage: the biophysical basis of immunoprotection by grafted methoxypoly(ethylene glycol) (mPEG). Acta Biomater. 6, 2631–2641.
Le Mire, L., Hollowood, K., Gray, D., Bordea, C., Wojnarowska, F., 2006. Melanomas in renal transplant recipients. Br. J. Dermatol. 154, 472–477.
Lee, S., Margolin, K., 2011. Cytokines in cancer immunotherapy. Cancers (Basel) 3, 3856–3893.
Lee, S.K., Lee, S.C., Kim, S.J., 2015. A novel cell-free strategy for promoting mouse liver regeneration: utilization of a conditioned medium from adipose-derived stem cells.

Hepatol. Int. 9, 310–320.
Lesterhuis, W.J., Haanen, J.B., Punt, C.J., 2011. Cancer immunotherapy–revisited. Nat. Rev. Drug Discov. 10, 591–600.
Liang, H., Zen, K., Zhang, J., Zhang, C.Y., Chen, X., 2013. New roles for microRNAs in cross-species communication. RNA Biol. 10, 367–370.
Liao, W., Lin, J.X., Leonard, W.J., 2011. IL-2 family cytokines: new insights into the complex roles of IL-2 as a broad regulator of T helper cell differentiation. Curr. Opin. Immunol. 23, 598–604.
Lichtenauer, M., Mildner, M., Hoetzenecker, K., Zimmermann, M., Podesser, B.K., Sipos, W., Berényi, E., Dworschak, M., Tschachler, E., Gyöngyösi, M., Ankersmit, H.J., 2011. Secretome of apoptotic peripheral blood cells (APOSEC) confers cytoprotection to cardiomyocytes and inhibits tissue remodelling after acute myocardial infarction: a preclinical study. Basic Res. Cardiol. 106, 1283–1297.
Maciel, R.M., Miki, S.S., Nicolau, W., Mendes, N.F., 1976. Peripheral blood T and B lymphocytes, in vitro stimulation with phytohemagglutinin, and sensitization with 2,4-dinitrochlorobenzene in Grave's disease. J. Clin. Endocrinol. Metab. 42, 583–587.
Mildner, M., Hacker, S., Haider, T., Gschwandtner, M., Werba, G., Barresi, C., Zimmermann, M., Golabi, B., Tschachler, E., Ankersmit, H.J., 2013. Secretome of peripheral blood mononuclear cells enhances wound healing. PLoS One 8, e60103.
Mullard, A., 2017. FDA approves first CAR t therapy. Nat. Rev. Drug Discov. 16, 669.
Murad, K.L., Gosselin, E.J., Eaton, J.W., Scott, M.D., 1999. Stealth cells: prevention of major histocompatibility complex class II-mediated T-cell activation by cell surface modification. Blood. 94, 2135–2141.
Nisbet, N.W., Simonsen, M., Zaleski, M., 1969. The frequency of antigen-sensitive cells in tissue transplantation. A commentary on clonal selection. J. Exp. Med. 129, 459–467.
Ockert, D., Schirrmacher, V., Beck, N., Stoelben, E., Ahlert, T., Flechtenmacher, J., Hagmüller, E., Buchcik, R., Nagel, M., Saeger, H.D., 1996. Newcastle disease virus-infected intact autologous tumor cell vaccine for adjuvant active specific immunotherapy of resected colorectal carcinoma. Clin. Cancer Res. 2, 21–28.
Perica, K., Varela, J.C., Oelke, M., Schneck, J., 2015. Adoptive T cell immunotherapy for cancer. Rambam Maimonides Med. J. 6, e0004.
Pileczki, V., Cojocneanu-Petric, R., Maralani, M., Neagoe, I.B., Sandulescu, R., 2016. MicroRNAs as regulators of apoptosis mechanisms in cancer. Clujul Med. 89, 50–55.
Punt, S., Fleuren, G.J., Kritikou, E., Lubberts, E., Trimbos, J.B., Jordanova, E.S., Gorter, A., 2015a. Angels and demons: Th17 cells represent a beneficial response, while neutrophil IL-17 is associated with poor prognosis in squamous cervical cancer. Oncoimmunology 4, e984539.
Punt, S., Langenhoff, J.M., Putter, H., Fleuren, G.J., Gorter, A., Jordanova, E.S., 2015b. The correlations between IL-17 vs. Th17 cells and cancer patient survival: a systematic review. Oncoimmunology 4, e984547.
Rabinovich, G.A., Toscano, M.A., 2009. Turning 'sweet' on immunity: galectin-glycan interactions in immune tolerance and inflammation. Nat. Rev. Immunol. 9, 338–352.
Renga, M., Pedrazzoli, P., Siena, S., 2003. Present results and perspectives of allogeneic non-myeloablative hematopoietic stem cell transplantation for treatment of human solid tumors. Ann. Oncol. 14, 1177–1184.
Schulof, R.S., Mai, D., Nelson, M.A., Paxton, H.M., Cox, J.W., Turner, M.L., Mills, M., Hix, W.R., Nochomovitz, L.E., Peters, L.C., 1988. Active specific immunotherapy with an autologous tumor cell vaccine in patients with resected non-small cell lung cancer. Mol. Biother. 1, 30–36.
Sholl-Franco, A., Araujo, E.G., 1997. Conditioned medium from activated spleen cells supports the survival of rat retinal cells in vitro. Braz. J. Med. Biol. Res. 30, 1299–1303.
Simader, E., Traxler, D., Kasiri, M.M., Hofbauer, H., Wolzt, M., Glogner, C., Storka, A., Mildner, M., Gouya, G., Geusau, A., Fuchs, C., Eder, C., Graf, A., Schaden, M., Golabi, B., Aretin, M.B., Suessner, S., Gabriel, C., Klepetko, W., Tschachler, E., Ankersmit, H.J., 2017. Safety and tolerability of topically administered autologous, apoptotic PBMC secretome (APOSEC) in dermal wounds: a randomized Phase 1 trial (MARSYAS I). Sci. Rep. 7, 6216.
Singh, R., Saini, N., 2012. Downregulation of BCL2 by miRNAs augments drug-induced apoptosis–a combined computational and experimental approach. J. Cell. Sci. 125, 1568–1578.
Starnes, C.O., 1992. Coley's toxins in perspective. Nature 357, 11–12.
Stenken, J.A., Poschenrieder, A.J., 2015. Bioanalytical chemistry of cytokines–a review. Anal. Chim. Acta 853, 95–115.
Suntharalingam, G., Perry, M.R., Ward, S., Brett, S.J., Castello-Cortes, A., Brunner, M.D., Panoskaltsis, N., 2006. Cytokine storm in a phase 1 trial of the anti-CD28 monoclonal antibody TGN1412. N. Engl. J. Med. 355, 1018–1028.
Thiele, S., Wittmann, J., Jäck, H.M., Pahl, A., 2012. miR-9 enhances IL-2 production in activated human CD4(+) T cells by repressing Blimp-1. Eur. J. Immunol. 42, 2100–2108.
Trickett, A., Kwan, Y.L., 2003. T cell stimulation and expansion using anti-CD3/CD28 beads. J. Immunol. Methods 275, 251–255.
Turchinovich, A., Burwinkel, B., 2012. Distinct AGO1 and AGO2 associated miRNA profiles in human cells and blood plasma. RNA Biol. 9, 1066–1075.
Valadi, H., Ekström, K., Bossios, A., Sjöstrand, M., Lee, J.J., Lötvall, J.O., 2007. Exosome-mediated transfer of mRNAs and microRNAs is a novel mechanism of genetic exchange between cells. Nat. Cell Biol. 9, 654–659.
Wang, D., Toyofuku, W.M., Chen, A.M., Scott, M.D., 2011. Induction of immunotolerance via mPEG grafting to allogeneic leukocytes. Biomaterials 32, 9494–9503.
Wang, D., Toyofuku, W.M., Scott, M.D., 2012. The potential utility of methoxypoly (ethylene glycol)-mediated prevention of rhesus blood group antigen RhD recognition in transfusion medicine. Biomaterials 33, 3002–3012.
Wang, D., Shanina, I., Toyofuku, W.M., Horwitz, M.S., Scott, M.D., 2015. Inhibition of autoimmune diabetes in NOD mice by miRNA therapy. PLoS One 10, e0145179.
Wilke, C.M., Kryczek, I., Wei, S., Zhao, E., Wu, K., Wang, G., Zou, W., 2011. Th17 cells in cancer: help or hindrance. Carcinogenesis 32, 643–649.
Yao, T., Asayama, Y., 2017. Animal-cell culture media: history, characteristics, and current issues. Reprod. Med. Biol. 16, 99–117.
Ye, J., Livergood, R.S., Peng, G., 2013. The role and regulation of human Th17 cells in tumor immunity. Am. J. Pathol. 182, 10–20.
Zheng, J.H., Nguyen, V.H., Jiang, S.N., Park, S.H., Tan, W., Hong, S.H., Shin, M.G., Chung, I.J., Hong, Y., Bom, H.S., Choy, H.E., Lee, S.E., Rhee, J.H., Min, J.J., 2017. Two-step enhanced cancer immunotherapy with engineered Salmonella typhimurium screting heterologous flagellin. Sci. Transl. Med. 9.
Zhou, M., Liu, Z., Zhao, Y., Ding, Y., Liu, H., Xi, Y., Xiong, W., Li, G., Lu, J., Fodstad, O., Riker, A.I., Tan, M., 2010. MicroRNA-125b confers the resistance of breast cancer cells to paclitaxel through suppression of pro-apoptotic Bcl-2 antagonist killer 1 (Bak1) expression. J. Biol. Chem. 285, 21496–21507.